Title
The role of the CD11c+ cells Tsc1-mTORC1 nutrient sensing pathway in metabolic homeostasis

Author
CHAGWEDERA, DANAI NYASHA

Publication Date
2018

Peer reviewed|Thesis/dissertation

The role of the CD11c+ cell Tsc1-mTORC1 nutrient sensing pathway in metabolic homeostasis.

by

Danai Nyasha Chagwedera

DISSERTATION

Submitted in partial satisfaction of the requirements for the degree of

DOCTOR OF PHILOSOPHY

in

Biomedical Sciences

in the

GRADUATE DIVISION

of the

UNIVERSITY OF CALIFORNIA, SAN FRANCISCO

Approved:

[redacted]

Committee in Charge

Dedicated to my dad, Tangai E. Chagwedera

Acknowledgements

Most importantly I would like to thank Ajay Chawla who took me in to his lab and has provided a stimulating and rigorous environment for me to learn and grow as a scientist. One thing that stands out most to me about Ajay is his fearlessness to delve into diverse research areas. Studying the microbiome is something I never imagined doing and was very scared when my results pointed me in that direction. However I am grateful to be in a lab where I was inspired to fearlessly follow the science and not confine myself to a certain area of research. I am grateful for the way Ajay has taught me to think and analyze data, ask questions and most importantly push scientific boundaries.

The Chawla lab is full of many fantastic current and former members. First I am grateful for my fellow graduate students Vassily Kutyavin and Yixuan Wu. These two have helped me grow as a scientists, have been there for me in tough times and have made being in the lab a pleasant experience. I am indebted to our lab manager, Xiaojin Cui for the many mice she has genotyped and orders she has placed. Former post-doc, Kirthana Ganeshan taught me how to work with mice and all the basic assays I know. Most importantly, I think we will all agree she was exemplary in being a role model in the lab for how to treat each other and create a truly supportive and collaborative environment even though we all worked on very different projects. Yew Ann Leong is our resident immunologist and I am so grateful for all his help and all that he has taught me. Thank you also to two new postdocs, Joni Nikkanen and Melissa Kinnebrew who I unfortunately did not overlap with much but have been truly fantastic to have around.

In a way I feel that I have had two lab experiences and that is because the Turnbaugh Lab has been so welcoming to me. I would like to thank them for bringing me in on their birthday celebrations, happy hours and lab meetings –it truly always brightened my day to work there –

the amazing views of Golden Gate Bridge were also a bonus of course. Thank you to Peter Turnbaugh who has been a phenomenal mentor and advisor to me. Thank you for the time spent on my project, teaching me and the many meetings and discussions we have had – you have helped shape me into the scientists I am today. A special thank you also to Qi Yan Ang and Jordan Bisanz who I collaborated with in Peter's Lab. Working with these two was a beautiful experience and I could not have asked for better collaborators. They taught me so much and I enjoyed working with them as a team.

My committee chair, Anita Sil is truly one of a kind and I am forever grateful she agreed to chair my committee. She has helped me navigate my PhD, provided invaluable advice, and is a major inspiration to me as a scientists and mentor. Thank you for all the time and energy spent on me – I hope I have made you proud. Ari Molofsky also served on my committee. Ari has an infectious energy and love for science and I am so grateful for all his input over the years – my project would not have taken form the way it did without his input.

I am indebted to the Biomedical Sciences Program and Medical Scientists Training Program at UCSF for all their support. Thank you to the directors Mark Ansel and Mark Anderson for their fantastic leadership, they truly put the well being of students first and it has been invaluable to belong to this program. A special thank you Demian, Ned, Geri, Amanda and Monique. I don't know how but somehow they make things run smoothly and make it looks easy from the outside. Thank you for your support and for being a great resource to us students.

Many thanks to my family who even though are all over the world have always encouraged me and provided me with the great foundation on which I now stand. Finally, I would like to thank my husband David Ikenna Adams who has supported me on this journey from the very start. Ikenna has proof-read every piece of work I have written from my qualifying

exam proposal to my F31 grant, and listened to many a practice talks. Even though science is not at all his language, he's only fallen asleep once during one of my practice talks. Thank you for keeping me calm and focused when I was angry and frustrated. Thank you for being patient and scheduling our lives around my lab hours. Most of all thank you for believing in me when I did not believe in myself.

Contributions to the Presented Work

Chapter 2.

Chapter 2 of this dissertation is work that is being prepared for submission as a manuscript. I performed all metabolic and immunologic assays in this Chapter under the guidance of Ajay Chawla. 16S sequencing, bomb calorimetry and Lactobacillus assays were performed with Qi Yan Ang, and Jordan Bisanz under the guidance of Peter Turnbaugh. Qi Yan Ang and Jordan Bisanz performed 16S sequencing analysis. Jingwei Cai performed short-chain fatty acid analysis under guidance from Andrew Patterson. Ajay Chawla and Peter Turnbaugh supervised the entirety of this work.

Chapter 3.

I performed all assays in this Chapter under the guidance of Ajay Chawla.

The role of the CD11c^{+} cell Tsc1-mTORC1 nutrient sensing pathway in metabolic homeostasis.

By. Danai Nyasha Chagwedera

Abstract

Alterations in host metabolic state have been reported to drastically alter gut microbial communities and influence host immune responses. While much attention has been paid to how the gut microbiome affects immune cell response, the reverse is understudied: how do immune cells influence the gut microbiome and in turn, regulate host metabolic state? CD11c^{+} cells are well known for their critical role in bridging innate and adaptive immune responses and are resident cells of almost all tissues in the body. In the gut, CD11c^{+} cells are located in the lamina propria and have been shown to play a key role in maintaining gut immune homeostasis. The tuberous sclerosis 1 - mechanistic target of rapamycin complex 1 (Tsc1-mTORC1) pathway is a cell's major nutrient-sensing pathway and functions to assess nutrient availability and determine whether energy-intensive processes, such as protein translation, should take place. Specifically, Tsc1 is a negative regulator of mTORC1 and inhibits mTOR activity under conditions of low nutrient availability. Given this knowledge, we asked whether perturbing nutrient sensing in CD11c^{+} cells would alter the gut microbiome to ultimately influence host systemic metabolism. We generated CD11c^{Cre} x Tsc1$^{flox/flox}$ mice (C57BL/6J background), where Tsc1 was specifically deleted in all CD11c expressing cells. Tsc1$^{flox/flox}$ ("control; CTRL") and CD11c^{Cre} x Tsc1$^{flox/flox}$ ("knockout; KO") mice were housed under thermoneutral (30°C) and sub-thermoneutral conditions (22°C), and placed on normal chow diet (NCD) or high-fat diet (HFD). Weight gain,

glucose and insulin sensitivity, and food intake were monitored over time. Additionally stool was collected for 16S rRNA gene sequencing. First, we determined how nutrient sensing by immune cells regulates body weight, adiposity and insulin action. Under all housing conditions, KO mice exhibited reduced weight gain as compared to CTRL mice. This decrease in body weight was not due to growth or birth defects and persisted with age. Analysis of food intake uncovered a reduction in overall food consumption. There were no differences in metabolic rate or physical activity between the groups. Interestingly, on a HFD protection from insulin resistance only occurred under thermoneutral conditions. In addition, we have investigated the microbial and immunologic mechanisms by which alterations in nutrient sensing in immune cells regulates weight gain. Flow cytometric analyses of immune cell populations in the small intestine and colon revealed differences in IgA binding. Co-housing experiments identified KO as capable of gaining weight in the presence of the CTRL mouse microbiome. We therefore show that activation of nutrient sensing pathways in $CD11c^+$ cells is sufficient to modulate systemic metabolism through alterations in the gut microbiome and that housing temperature conditions affects insulin and the microbiome. This project furthers our understanding of the role immune cells play in regulating systemic metabolism and has immediate translational implications for the treatment of metabolic disorders.

Table of Contents

List of Figures

Chapter 1

Chapter 2

Chapter 3

CHAPTER 1: INTRODUCTION

How is energy balance and weight gain controlled? In 1953 Kennedy proposed a unique system where by the brain is informed of available energy stores via circulating signals and in response to these signals adjusts food intake (Kennedy, 1953). This is known as the energy homeostasis system and is composed of signals to the brain that determine whether, when and how much to eat. The neurocircuitry in the brain is composed of orexigenic and anorexigenic hypothalamic neurons expressing agouti-related protein (AGRP) and pro-opiomelanocortin (POMC). We now know that many factors feed in to this neurocircuitry. These factors can be broadly dived into adiposity signals (leptin and insulin), gut peptides, (PYY, GLP-1, CCK, ghrelin), nutrients and even pro-inflammatory cytokines (interleukin-6 and tumor necrosis factor-α) (Figure 1.1) (Morton et al., 2014). Although there are many factors known to contribute to this energy homeostasis circuit, our understanding of this is not complete, in particular the role the immune system plays in regulating energy homeostasis and weight control under normal non-obese conditions is a mystery.

A recent explosion in the field of immunometabolism has given us a clue into the types of immune cells and pathways that play a role in regulating energy homeostasis in a diseased state. During obesity, significant changes occur in the epididymal fat pad that lead to metabolic dysregulation. Adipocyte cells hypertrophy, leading to local hypoxia and a significant change in the immune cell milieu, in particular an infiltration of Th1 $CD4^+$ T, B, $CD8^+$ T, mast cells, macrophages ($CD11c^+$) and neutrophils (Figure 1.2) (Lackey and Olefsky, 2016) .

Although many immune cells have been shown to contribute to high-fat diet induced metabolic dysfunction, none are as instrumental as the $CD11c^+$ cell. CD11c is traditionally thought of as a being on the surface of macrophages and dendritic cells (Abram et al., 2014),

although in CD11c-cre mice, some deletion has been shown in populations of monocytes, NK cells as well as low level, non-specific deletion in T and B cells.

The role of $CD11c^+$ cells in high-fat diet induced metabolic dysfunction is instrumental - up to 40% of resident cells in obese tissue can be CD11c positive. $CD11c^+$ macrophages are specifically recruited to adipose tissue when mice are exposed to a high-fat diet (Lumeng et al., 2007; Nguyen et al., 2007). These $CD11c^+$ cells are pro-inflammatory, expressing IL-1β, IL-6, TNF-α and CCR2, leading to subsequent low-grade inflammation induced insulin resistance (Greenberg and Obin, 2006; Shoelson et al., 2006). Ablation of $CD11c^+$ cells using CD11c-DTR mice results in normalization of insulin sensitivity and a decrease in local and systemic inflammatory makers (Patsouris et al., 2008). Additionally, under homeostatic conditions, CD11c is also found on the surface of a small number of microglia – the main immune cells of brain (Immig et al., 2015; Prodinger et al., 2011; Wlodarczyk et al., 2014). Microglia play an important role in regulating food consumption and weight gain through modulation of hypothalamic inflammation (Thaler et al., 2013; Valdearcos et al., 2017).

Given the important roles of $CD11c^+$ cells in energy homeostasis and weight gain we asked what the effect of altering a metabolic pathway in $CD11c^+$ cells would be on systemic metabolism. In particular we specifically deleted Tsc1 in $CD11c^+$ cells by creating a $Tsc1^{f/f}$ x $CD11c^{Cre}$ mouse.

The Tsc1-mTORC1 pathway is a central regulator of cell metabolism (Figure 1.3). The tuberous sclerosis complex 1 is a negative regulator of mammalian target of rapamycin complex 1. Activation of the Tsc1-mTORC1 pathway results in energy requiring processes such as protein translation, cell growth and metabolism to occur. The Tsc1-mTORC1 pathway has recently

emerged as playing an important role in CD11c^{+} cell biology (Shimobayashi and Hall, 2014; Laplante et al., 2012; Weichhart et al., 2015).

Activation of mTORC1 in CD11c^{+} cells by targeted deletion of Tsc1 (Tsc1$^{f/f}$ CD11c^{Cre}) affects CD11c^{+} cell function, maturation and differentiation (Amiel et al., 2014; Luo et al., 2017; Pan et al., 2013; Sathaliyawala et al., 2010; Sukhbaatar et al., 2016; Wang and Res, 2014). Tsc1 ablation in CD11c^{+} cells results in upregulation of genes involved in cell survival, proliferation, metabolism (Luo et al., 2018). Three studies have examined the functional role of Tsc1 in CD11c^{+} cells *in vivo*. The diversity of their findings points to the complexity and importance of the Tsc1-mTORC1 pathway in CD11c^{+} cells. Pan et al show Tsc1-deficient CD11c^{+} cells have defective antigen presentation to CD4^{+} T cells due to altered cytokine expression and impaired CIITA/MHC-II expression (Pan et al., 2013). Wang et al demonstrated a disruption in dendritic cell development resulting in reduced numbers in mesenteric lymph node, liver and kidney CD11c^{+} cells. They also observed decreased IL-12p35 production resulting in reduced Th1stimulation, despite elevated maturation markers (CD86, CD80, CD40) (Wang et al., 2013). Luo et al did not detect alterations in co-stimulatory molecules, differentiation or cytokine expression but did note defective antigen-specific response both *in vitro* and *in vivo.* In addition, they observed characteristics of autoimmunity such as increased naïve T cell proliferation, splenomegaly, lymphadenopathy, increased serum immunoglobin levels and weight loss (Luo et al., 2017).

Although our initial studies of CD11c^{+} cells were motivated by the role of CD11c^{+} cells in obese animals we found to our surprise that the phenotype of reduced weight gain in Tsc1$^{f/f}$CD11c^{Cre} mice was independent of high-fat diet and thus CD11c^{+} cells in epididymal fat

pads. We therefore turned out attention to other areas in the body where $CD11c^+$ cells are present and could impact systemic metabolism.

In the intestine, CD11c is expressed on mononuclear phagocytes (MPs) which comprise both macrophages and dendritic cells (Bradford et al., 2011; Cerovic et al., 2014) (Figure 1.4). MPs can affect the intestinal microbial composition and gut homeostasis in several ways. Intestinal dendritic cells sample luminal content via specialized microfold M cells, through extension of protrusions through the epithelial layer or via transport of luminal antigen in goblet cells (Farache et al., 2013). Intestinal macrophages can sample luminal content via transepithelial dendrites (Chieppa et al., 2006; Niess et al., 2005). Once the antigen is acquired, MP's can trigger the innate and adaptive immune response. $CD103^+$ DCs have a unique ability to induce a tolerogenic response by migrating to the mesenteric lymph node and inducing differentiation of $Foxp3^+$ T regulatory (Treg) cells (Sun et al., 2007; Coombes et al., 2007). In addition, macrophages play an important role in maintenance and secondary expansion of these Tregs (Hadis et al., 2011). Macrophages also play a key role in supporting gut barrier integrity (Pull et al., 2005; Qualls et al., 2006). This is evidenced by the fact that $CD11c^+$ cells deficient in mTORC1 activity have reduced IL-10 secretion and are highly susceptible to dextran sodium sulfate-induced colitis (Ohtani et al., 2012). Finally, macrophages possess a high phagocytic and bactericidal activity that can directly clear microbes (Müller et al., 2012). These roles collectively have a great effect on the microbiome which led us to hypothesize that $CD11c^+$ cells were altering the microbiome in our model which in turn was regulating energy homeostasis.

Several key studies have shown that the gut microbiome regulation of host energy homeostasis and weight gain. The first observation that the microbiome modulates host metabolism came from Bäckhead et al who showed that within 14 days of colonization, germ-

free mice had a 60% increase in body fat content and developed insulin resistance (Bäckhed et al., 2004). It was then appreciated that obesity drastically alters the gut microbiome composition and Turnbaugh et al showed that microbiota from obese mice was sufficient to confer weight gain to germ-free recipient mice (Ley et al., 2005; Turnbaugh et al., 2006). These seminal observations, have led to an understanding of the mechanisms by which the microbiome regulates host metabolism. Directly, the microbiome can alter host metabolism by regulating fermentation and energy harvest from food. Indirectly, microbial products such as lipopolysaccharides, peptidoglycan, bile acids and short-chain fatty acids can affect the liver, brain, muscle and adipose tissue which subsequently influence host metabolism (Tremaroli and Nature, 2012).

This dissertation connects the worlds of immunology, metabolism and the microbiome. Here, we examine the effect of altering the central regulator of metabolism Tsc1-mTORC1 pathway in $CD11c^{+}$ cells on systemic metabolism. Our findings provide evidence that altering immune cell metabolism is sufficient to alter host systemic metabolism through specific changes in gut microbiome populations.

FIGURES

Figure 1.1 The energy homeostasis system connects to neurocircuitry to control food intake. Peptide YY (PYY) and ghrelin feed in to orexigenic neuron Agouti-related Peptide (AgRP). Leptin, insulin, pro-inflammatory cytokines, nutrients, Glucagon-Like Peptide-1 (GLP-1), and Cholecystokinin (CCK) all feed into anorexigenic neuron Pro-opiomelanocortin (POMC). AgRP and POMC neurons stimulate effector neurons in the Paraventricular nucleus (PVN).

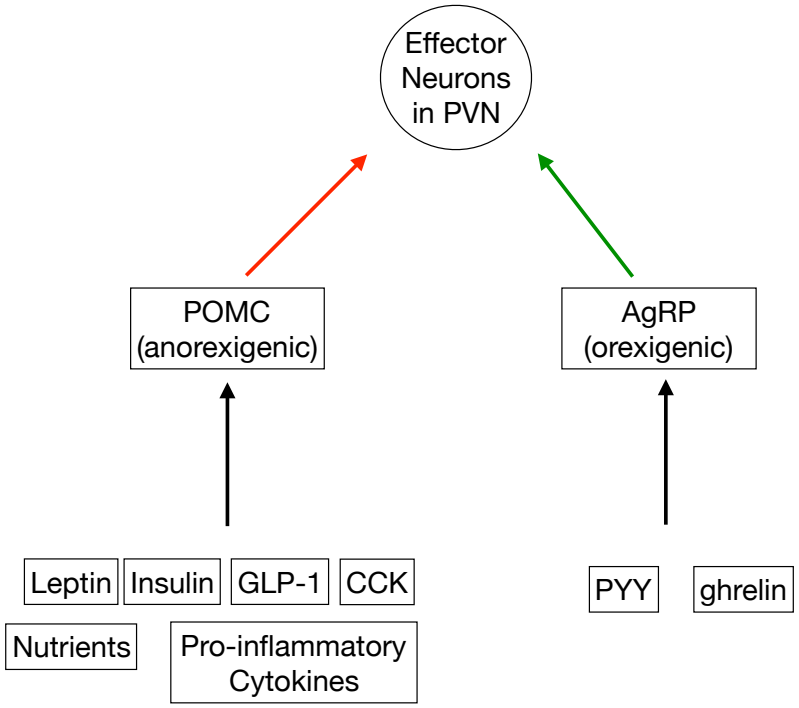

Figure 1.1 The energy homeostasis system connects to neurocircuitry to control food intake.

Figure 1.2 Immune cell and adipocyte changes when moving from lean to obese state. In the lean state anti-inflammatory cytokines from resident immune cells and alternatively-activated macrophages (AAM) promote insulin sensitivity. In the obese state adipocytes hypertrophy causing hypoxia. $CD11c^+$ cells, also called classically-activated macrophages (CAMs) infiltrate the fat pads and secrete pro-inflammatory cytokines which leads to insulin-resistance.

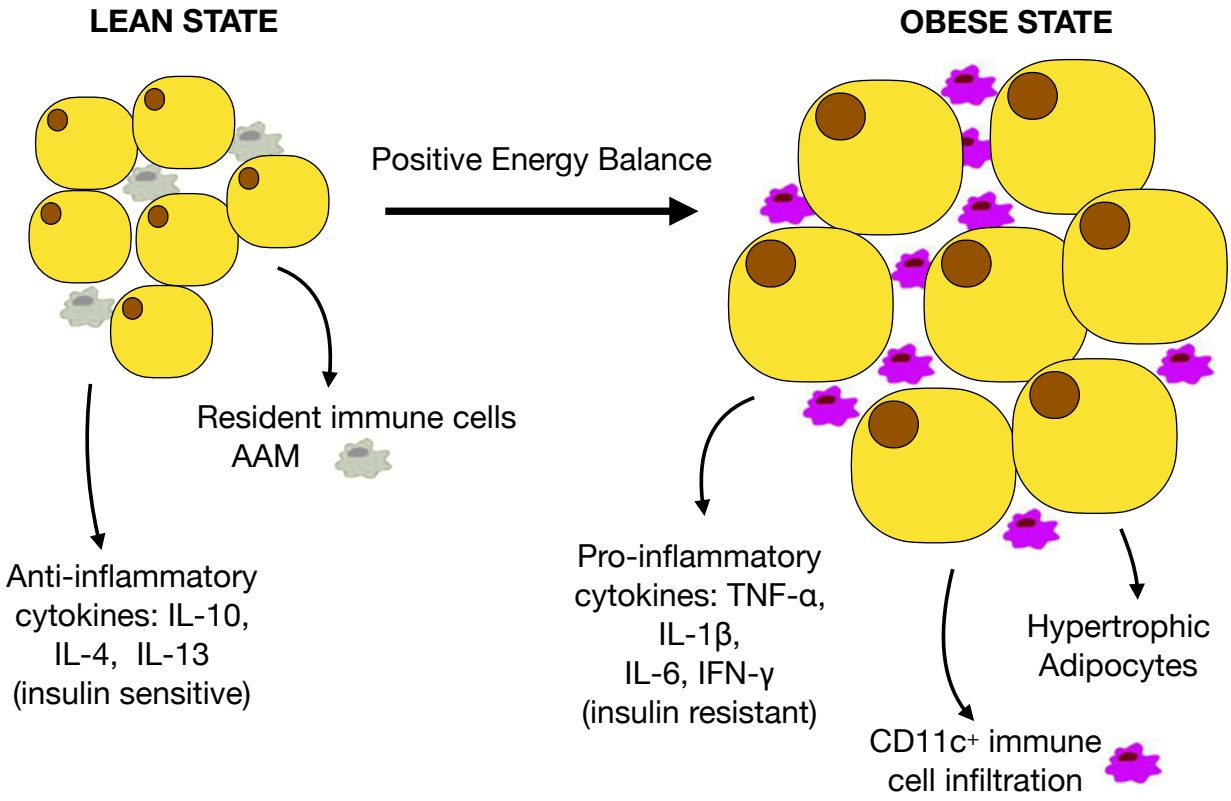

Figure 1.2 Immune cell and adipocyte changes when moving from lean to obese state

Figure 1.3 The Tsc1-mTORC1 pathway. Nutrients, growth factors and energy activate the Tsc1-mTORC1 pathway. Tuberous Sclerosis Protein 1 (Tsc1) forms a heterodimer with Tsc2 and together they inhibit Ras Homolog Enriched in Brain (Rheb) bound GTP – an activator of mammalian target of rapamycin complex 1 (mTORC1). Activated mTORC1 promotes protein synthesis and inhibits autophagy to promote cell growth, division and differentiation in response to the available energy.

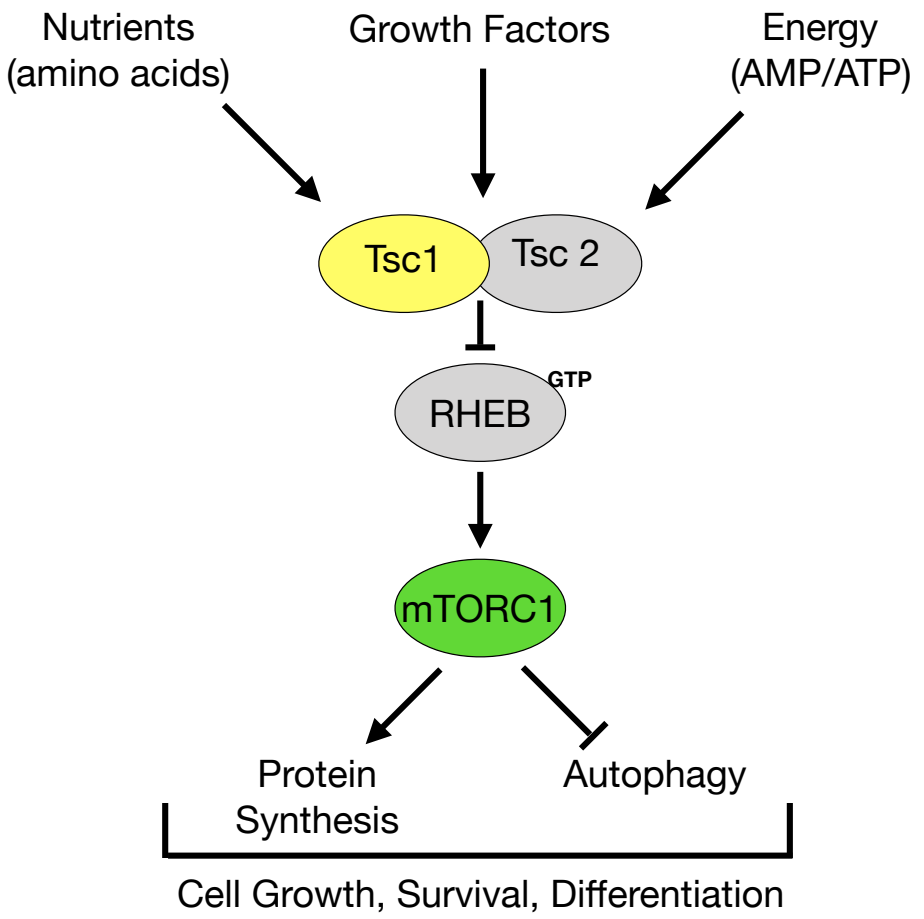

Figure 1.3 The Tsc1-mTORC1 pathway.

Figure 1.4 Role of macrophages and dendritic cells in the intestine. CD11c is found on the surface of both macrophages and dendritic cells in the intestine. Intestinal macrophages (left) engulf invading bacteria, maintain epithelial barrier integrity and support secondary expansion of T regulatory (Treg) cells. Dendritic cells (right) use dendrites to sample luminal contents and then migrate to the mesenteric lymph node where they stimulate the appropriate T-cell response.

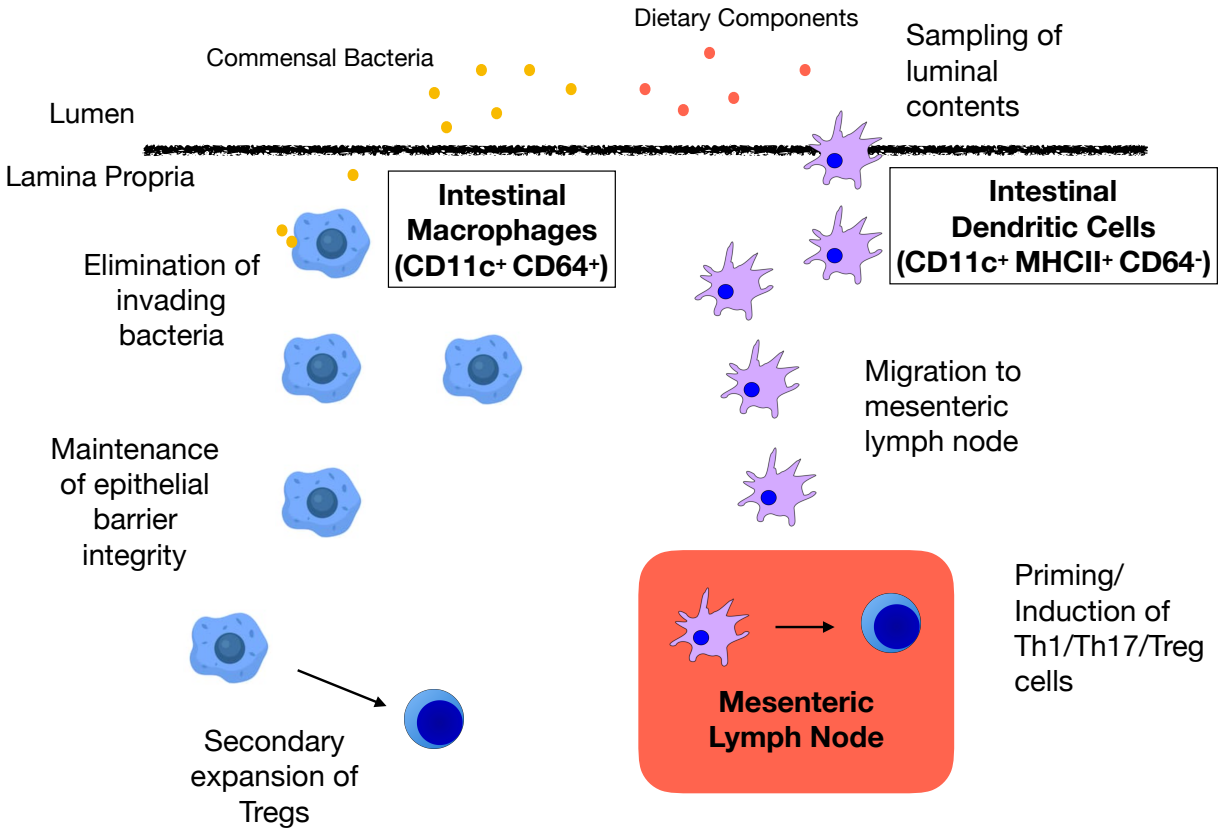

Figure 1.4 Role of macrophages and dendritic cells in the intestine.

REFERNCES

Abram, Clare L., et al. "Comparative analysis of the efficiency and specificity of myeloid-Cre deleting strains using ROSA-EYFP reporter mice." *Journal of immunological methods* 408 (2014): 89-100.

Amiel, Eyal, et al. "Mechanistic target of rapamycin inhibition extends cellular lifespan in dendritic cells by preserving mitochondrial function." *The Journal of Immunology* (2014): 1302498.

Bäckhed, Fredrik, et al. "The gut microbiota as an environmental factor that regulates fat storage." *Proceedings of the national academy of sciences* 101.44 (2004): 15718-15723.

Bradford, Barry M., et al. "Defining the anatomical localisation of subsets of the murine mononuclear phagocyte system using integrin alpha X (Itgax, CD11c) and colony stimulating factor 1 receptor (Csf1r, CD115) expression fails to discriminate dendritic cells from macrophages." *Immunobiology* 216.11 (2011): 1228-1237.

Cerovic, Vuk, et al. "Intestinal macrophages and dendritic cells: what's the difference?." *Trends in immunology* 35.6 (2014): 270-277.

Chieppa, Marcello, et al. "Dynamic imaging of dendritic cell extension into the small bowel lumen in response to epithelial cell TLR engagement." *Journal of Experimental Medicine*203.13 (2006): 2841-2852.

Coombes, Janine L., et al. "A functionally specialized population of mucosal CD103+ DCs induces Foxp3+ regulatory T cells via a TGF-β–and retinoic acid–dependent mechanism." *Journal of Experimental Medicine* 204.8 (2007): 1757-1764.

Farache, Julia, et al. "Luminal bacteria recruit CD103+ dendritic cells into the intestinal epithelium to sample bacterial antigens for presentation." *Immunity* 38.3 (2013): 581-595.

Greenberg, Andrew S., and Martin S. Obin. "Obesity and the role of adipose tissue in inflammation and metabolism–." *The American journal of clinical nutrition* 83.2 (2006): 461S-465S.

Hadis, Usriansyah, et al. "Intestinal tolerance requires gut homing and expansion of FoxP3+ regulatory T cells in the lamina propria." *Immunity* 34.2 (2011): 237-246.

Immig, Kerstin, et al. "CD11c-positive cells from brain, spleen, lung, and liver exhibit site-specific immune phenotypes and plastically adapt to new environments." *Glia* 63.4 (2015): 611-625.

Kennedy, G. C. "The role of depot fat in the hypothalamic control of food intake in the rat." *Proc. R. Soc. Lond. B*140.901 (1953): 578-592.

Lackey, Denise E., and Jerrold M. Olefsky. "Regulation of metabolism by the innate immune system." *Nature Reviews Endocrinology* 12.1 (2016): 15.

Laplante, Mathieu, and David M. Sabatini. "mTOR signaling in growth control and disease." *Cell* 149.2 (2012): 274-293.

Ley, Ruth E., et al. "Obesity alters gut microbial ecology." *Proceedings of the National Academy of Sciences* 102.31 (2005): 11070-11075.

Lumeng, Carey N., Jennifer L. Bodzin, and Alan R. Saltiel. "Obesity induces a phenotypic switch in adipose tissue macrophage polarization." *The Journal of clinical investigation*117.1 (2007): 175-184.

Luo, Yuechen, et al. "Tsc1 expression by dendritic cells is required to preserve T-cell homeostasis and response." *Cell death & disease* 8.1 (2017): e2553.

Luo, Yuechen, et al. "Tsc1-dependent transcriptional programming of dendritic cell homeostasis and function." *Experimental cell research* 363.1 (2018): 73-83.

Morton, Gregory J., Thomas H. Meek, and Michael W. Schwartz. "Neurobiology of food intake in health and disease." *Nature Reviews Neuroscience* 15.6 (2014): 367.

Müller, Andreas J., et al. "Salmonella gut invasion involves TTSS-2-dependent epithelial traversal, basolateral exit, and uptake by epithelium-sampling lamina propria phagocytes." *Cell host & microbe* 11.1 (2012): 19-32.

Niess, Jan Hendrik, et al. "CX3CR1-mediated dendritic cell access to the intestinal lumen and bacterial clearance." *Science* 307.5707 (2005): 254-258.

Ohtani, Masashi, et al. "Cutting edge: mTORC1 in intestinal CD11c+ CD11b+ dendritic cells regulates intestinal homeostasis by promoting IL-10 production." *The Journal of Immunology* (2012): 1200069.

Nguyen, MT Audrey, et al. "A subpopulation of macrophages infiltrates hypertrophic adipose tissue and is activated by free fatty acids via Toll-like receptors 2 and 4 and JNK-dependent pathways." *Journal of Biological Chemistry* 282.48 (2007): 35279-35292.

Pan, Hongjie, et al. "Critical role of the tumor suppressor tuberous sclerosis complex 1 in dendritic cell activation of CD4 T cells by promoting MHC class II expression via IRF4 and CIITA." *The Journal of Immunology* (2013): 1201443.

Patsouris, David, et al. "Ablation of CD11c-positive cells normalizes insulin sensitivity in obese insulin resistant animals." *Cell metabolism* 8.4 (2008): 301-309.

Prodinger, Carolin, et al. "CD11c-expressing cells reside in the juxtavascular parenchyma and extend processes into the glia limitans of the mouse nervous system." *Acta neuropathologica*121.4 (2011): 445-458.

Pull, Sarah L., et al. "Activated macrophages are an adaptive element of the colonic epithelial progenitor niche necessary for regenerative responses to injury." *Proceedings of the National Academy of Sciences* 102.1 (2005): 99-104.

Qualls, Joseph E., et al. "Suppression of experimental colitis by intestinal mononuclear phagocytes." *Journal of leukocyte biology* 80.4 (2006): 802-815.

Sathaliyawala, Taheri, et al. "Mammalian target of rapamycin controls dendritic cell development downstream of Flt3 ligand signaling." *Immunity* 33.4 (2010): 597-606.

Shimobayashi, Mitsugu, and Michael N. Hall. "Making new contacts: the mTOR network in metabolism and signalling crosstalk." *Nature reviews Molecular cell biology* 15.3 (2014): 155.

Shoelson, Steven E., Jongsoon Lee, and Allison B. Goldfine. "Inflammation and insulin resistance." *The Journal of clinical investigation* 116.7 (2006): 1793-1801.

Sukhbaatar, Nyamdelger, Markus Hengstschläger, and Thomas Weichhart. "mTOR-mediated regulation of dendritic cell differentiation and function." *Trends in immunology* 37.11 (2016): 778-789.

Sun, Cheng-Ming, et al. "Small intestine lamina propria dendritic cells promote de novo generation of Foxp3 T reg cells via retinoic acid." *Journal of Experimental Medicine* 204.8 (2007): 1775-1785.

Thaler, Joshua P., et al. "Hypothalamic inflammation: marker or mechanism of obesity pathogenesis?." *Diabetes* 62.8 (2013): 2629-2634.

Turnbaugh, Peter J., et al. "An obesity-associated gut microbiome with increased capacity for energy harvest." *nature* 444.7122 (2006): 1027.

Tremaroli, Valentina, and Fredrik Bäckhed. "Functional interactions between the gut microbiota and host metabolism." *Nature* 489.7415 (2012): 242.

Valdearcos, Martin, et al. "Microglial inflammatory signaling orchestrates the hypothalamic immune response to dietary excess and mediates obesity susceptibility." *Cell metabolism*26.1 (2017): 185-197.

Wang, Yanyan, and Hongbo Chi. "mTOR signaling and dendritic cell biology." *J Immunol Clin Res* 2.1 (2014): 1015.

Wang, Yanyan, et al. "Tuberous sclerosis 1 (Tsc1)-dependent metabolic checkpoint controls development of dendritic cells." *Proceedings of the National Academy of Sciences* 110.50 (2013): E4894-E4903.

Weichhart, Thomas, Markus Hengstschläger, and Monika Linke. "Regulation of innate immune cell function by mTOR." *Nature Reviews Immunology* 15.10 (2015): 599.

Wlodarczyk, Agnieszka, et al. "Comparison of microglia and infiltrating CD11c+ cells as antigen presenting cells for T cell proliferation and cytokine response." *Journal of neuroinflammation* 11.1 (2014): 57.

CHAPTER 2.

Nutrient sensing in CD11c cells alters the gut microbiome to regulate food intake and body mass.

Nutrient sensing in CD11c cells alters the gut microbiome to regulate food intake and body mass

Authors: D. Nyasha Chagwedera[1], Qi Yan Ang[2], Jordan E. Bisanz[2], Kirthana Ganeshan[1], Jingwei Cai[3], Andrew D. Patterson[3], Peter J. Turnbaugh[2,5], and Ajay Chawla[1,4,5]

Affiliations:

[1]Cardiovascular Research Institute, University of California, San Francisco, 94143-0795, USA

[2]Department of Microbiology & Immunology, University of California San Francisco (UCSF), San Francisco, CA 94143, USA.

[3]Center for Molecular Toxicology and Carcinogenesis, Department of Veterinary and Biomedical Sciences, The Pennsylvania State University, University Park, Pennsylvania, 16802, USA.

[4]Departments of Physiology and Medicine, University of California, San Francisco, 94143-0795, USA

[5]These authors contributed equally to this work

Correspondence: peter.turnbaugh@ucsf.edu and ajay.chawla@ucsf.edu

ABSTRACT

Microbial dysbiosis and inflammation are implicated in the pathogenesis of diet-induced obesity and insulin resistance. However, it is not known whether crosstalk between immunity and the microbiome also regulates metabolic homeostasis in healthy animals. Here, we report that genetic deletion of *Tsc1* in CD11c cells ($Tsc1^{f/f}CD11c^{Cre}$ mice) reduced food intake and body mass in the absence of metabolic disease. Cohousing and fecal transplant experiments revealed a dominant role for the host microbiome in regulation of body weight. 16S rRNA sequencing, selective culture, and reconstitution experiments further confirmed that selective deficiency of *Lactobacillus* strain Q1-7 contributed to decreased food intake and body mass in $Tsc1^{f/f}CD11c^{Cre}$ mice. Mechanistically, activation of mTORC1 signaling in CD11c cells regulated production of *Lactobacillus* strain Q1-7-specific IgA, allowing for its stable colonization in the gut. Together, our findings reveal an unexpected transkingdom immune-microbiome feedback loop for homeostatic regulation of food intake and body mass in mammals.

INTRODUCTION

Hypothalamic circuits regulate caloric intake, meal size, and energy expenditure to maintain body weight within a narrow range (Morton et al., 2014; Waterson and Horvath, 2015). This is principally mediated by the crosstalk between orexigenic and anorexigenic hypothalamic neurons expressing agouti-related protein (AGRP) and pro-opiomelanocortin (POMC), respectively. Since the activity of these neurons can be modulated by hormones (leptin, insulin, and glucagon-like peptide 1 (GLP1)), nutrients (glucose and fatty acids), and inflammatory cytokines (interleukin-6 and tumor necrosis factor-α), it provides a mechanism for regulating food intake and body weight under diverse set of dietary and environmental conditions.

In addition to these classical neuronal and hormonal pathways, previous studies in obese animals have implicated the immune system and the microbiome in regulation of body weight and insulin action (Heiss and Olofsson, 2018; Hotamisligil, 2017; Lee et al., 2018; Man et al., 2017; Maruvada et al., 2017; Schroeder and Backhed, 2016; Sonnenburg and Backhed, 2016). For example, obesity is associated with accumulation of $CD11c^+$ cells in white adipose tissue and microglial activation in the hypothalamus, which contribute to local and systemic inflammation, peripheral insulin resistance, and weight gain (Lumeng et al., 2007; Patsouris et al., 2008; Valdearcos et al., 2017). Moreover, in both mice and humans, dietary obesity alters the composition of the microbiome to increase energy harvest and systemic inflammation, factors which favor weight gain and insulin resistance, respectively (Ley et al., 2005; Nicholson et al., 2012; Turnbaugh et al., 2009; Turnbaugh et al., 2006). While these studies in obese animals demonstrate a pathogenic role for inflammation and microbial dysbiosis in metabolic diseases, the physiologic importance of these transkingdom interactions in healthy animals remains less well understood.

Here, we tested the hypothesis that nutrient sensing in innate immune cells regulates energy balance under physiologic conditions. We found that genetic activation of mechanistic target of rapamycin complex 1 (mTORC1) in CD11c cells, as in $Tsc1^{f/f}CD11c^{Cre}$ mice, alters the gut microbiome to reduce food intake and body weight in lean mice. Because these metabolic phenotypes were transmissible by the microbiome, in particular by *Lactobacillus* strain Q1-7, our findings suggest existence of transkingdom immune-microbiome circuits for homeostatic regulation of food intake and body mass in healthy animals.

RESULTS

Activation of mTORC1 signaling in CD11c cells reduces body mass and food intake

To investigate whether mTOR signaling in CD11c cells regulates glucose and energy homeostasis, we generated mice in which Tsc1, an inhibitor of the mTORC1 complex (Gonzalez and Hall, 2017; Saxton and Sabatini, 2017), was selectively deleted in CD11c cells (designated $Tsc1^{f/f}CD11c^{Cre}$ mice). Deletion of Tsc1 activated mTORC1 signaling in CD11c cells, as evidenced by increased phosphorylation of its downstream target S6 (Figure S1A-C). Although previous studies have implicated CD11c cells in pathogenesis of obesity-associated insulin resistance (Lumeng et al., 2007; Patsouris et al., 2008), nearly all of this work has been performed in animals housed under thermal stress conditions (ambient temperature (T_a) of 20-22°C). Since we and others have reported that thermal stress has a profound effect on systemic metabolism (Cannon and Nedergaard, 2011; Ganeshan and Chawla, 2017; Gordon, 2017; Tian et al., 2016), we performed all of our studies with mice housed at thermoneutrality (T_a = 30°C). We observed that, compared to their littermate controls ($Tsc1^{f/f}$ mice), thermoneutral $Tsc1^{f/f}CD11c^{Cre}$ mice gained less weight on a high fat diet (Figure 1A), which was not associated with improvements in glucose tolerance or insulin sensitivity (Figure 1B, C). These results suggested

that the primary metabolic effects stemming from mTORC1 activation in CD11c cells were likely to be on body mass. To test this hypothesis, we repeated the studies with $Tsc1^{f/f}$ and $Tsc1^{f/f}CD11c^{Cre}$ mice that were fed a low-fat regular chow diet (24.5% protein, 13.1% fat, and 62.3% carbohydrates). We again observed that $Tsc1^{f/f}CD11c^{Cre}$ mice had a lower body mass, which was independent of linear growth (Figure 1D and Figure S1D). Dual-energy X-ray absorptiometry (DEXA) revealed that reduction in both lean and fat mass contributed to the observed decrease in body mass in $Tsc1^{f/f}CD11c^{Cre}$ mice (Figure 1E). Based on these observations, we chose to study the systemic effects of mTORC1 activation in CD11c using mice that were fed a low-fat regular chow diet, which allowed us to avoid the pleiotropic effects of high fat diets on metabolic and immune systems, and the gut microbiome.

To identify the underlying mechanisms for the observed decrease in body mass, we quantified changes in energy expenditure in $Tsc1^{f/f}$ and $Tsc1^{f/f}CD11c^{Cre}$ mice. We found that oxygen consumption and locomotor activity were similar in both groups of mice (Figure 1F, G and Figure S1E). Consistent with these observations, expression of thermogenic genes and thermogenic protein uncoupling protein 1 (UCP1) was not significantly different between the genotypes in brown adipose tissue (Figure S1F, G). We next asked whether deletion of Tsc1 in CD11c cells affected energy intake or absorption. Measurement of food intake revealed that food consumption was reduced by ~22% in $Tsc1^{f/f}CD11c^{Cre}$ mice (Figure 1H), whereas bomb calorimetry revealed that energy harvest was similar in both groups of mice (Figure 1I). This observed reduction in food intake was independent of systemic inflammation, hypothalamic microglial activation, and intestinal histology, barrier function, and inflammation (Figure 1J, K and S2A-F), suggesting that other factors contribute to decreased food intake and smaller body mass in $Tsc1^{f/f}CD11c^{Cre}$ mice.

The microbiome of Tsc1$^{f/f}$CD11c^{Cre} mice reduces food intake and body mass

The gut microbiome is an important factor that regulates energy homeostasis. In mice, maternal transfer of the microbiome occurs at birth, which undergoes diversification and stabilization as animals wean from breast milk to solid food (Stappenbeck and Virgin, 2016). Because we observed that body mass of Tsc1$^{f/f}$CD11c^{Cre} mice diverged from their littermate controls shortly after weaning (Figure 2A), we postulated that differences in the structure and function of gut microbial communities found in Tsc1$^{f/f}$ and Tsc1$^{f/f}$CD11c^{Cre} mice might contribute to energy homeostasis. In support of this hypothesis, when Tsc1$^{f/f}$ and Tsc1$^{f/f}$CD11c^{Cre} mice were cohoused instead of being separated at weaning, body mass, body composition, and food intake were not significantly different between the genotypes (Figure 2B-D). These differences in food intake and body weight between separated and cohoused Tsc1$^{f/f}$ and Tsc1$^{f/f}$CD11c^{Cre} mice could not be accounted for by variations in circulating levels of anorexigenic hormones leptin and GLP-1 (Figure S3A-C). These findings together suggested that the different microbial communities of Tsc1$^{f/f}$ and Tsc1$^{f/f}$CD11c^{Cre} mice might contribute to the observed differences in food intake and body mass.

Principal Coordinates Analysis (PCoA) of 16S rRNA sequence variants using Bray-Curtis dissimilarities revealed that microbial communities were compositionally distinct between Tsc1$^{f/f}$ and Tsc1$^{f/f}$CD11c^{Cre} mice when they were housed separately (Figure 2E and Figure S3D). However, these differences in microbial composition disappeared when the two genotypes were cohoused (Figure 2E and Figure S3D), which coincided with lack of difference in body mass between the genotypes (Figure 2B). Furthermore, analysis of sequence variants across three replicate experiments revealed four clades, including *Lactobacillaceae*, *Muribaculaceae*, *Lachnospiraceae* and *Ruminococcaceae*, that were increased or decreased in Tsc1$^{f/f}$CD11c^{Cre}

mice compared to Tsc1$^{f/f}$ mice (Figure 2F). Because the shifts in microbial composition paralleled the changes in food intake, it suggested a dominant role for the host microbiome in regulation of body mass. We tested this hypothesis by oral gavage of C57BL/6J mice, which were pretreated with antibiotics, with microbiota from Tsc1$^{f/f}$ or Tsc1$^{f/f}$CD11c^{Cre} mice. We observed that C57BL/6J mice receiving microbiota from Tsc1$^{f/f}$CD11c^{Cre} mice had lower food intake and body mass than those gavaged with microbiota from Tsc1$^{f/f}$ mice (Figure 2G, H). Together, these data suggest that Tsc1$^{f/f}$ and Tsc1$^{f/f}$CD11c^{Cre} mice harbor distinct microbial communities, whose adoptive transfer into C57BL/6J mice is sufficient to alter food intake and body mass.

Relative abundance of *Lactobacillus johnsonii* group is reduced in microbiota of Tsc1$^{f/f}$CD11c^{Cre} mice

To narrow down the specific microbial taxa responsible for the regulation of the body mass in Tsc1$^{f/f}$CD11c^{Cre} mice, we performed two types of microbiome chase experiments. First, we asked whether transfer of Tsc1$^{f/f}$ mice to dirty cages, which previously housed Tsc1$^{f/f}$CD11c^{Cre} mice, affected weight gain in Tsc1$^{f/f}$ mice (Figure 3A). We observed that the rate of change in body mass and food intake was not significantly different between Tsc1$^{f/f}$ mice transferred to clean or Tsc1$^{f/f}$CD11c^{Cre} dirty cages (Figure 3B, C). Second, we asked whether transfer of Tsc1$^{f/f}$CD11c^{Cre} mice to cages that previously housed Tsc1$^{f/f}$ mice might promote an increase in body mass (Figure 3D). Compared to control mice, we found that the rate of weight gain and food intake increased when Tsc1$^{f/f}$CD11c^{Cre} mice were transferred to dirty cages that previously housed Tsc1$^{f/f}$ mice (Figure 3E, F). Similar changes in body mass and food consumption were observed when Tsc1$^{f/f}$CD11c^{Cre} mice were gavaged with donor microbiota from Tsc1$^{f/f}$ mice for 8 weeks (Figure 3G, H). Together, these data suggest that adoptive transfer

of $Tsc1^{f/f}$ microbiome is sufficient to rescue weight gain in $Tsc1^{f/f}CD11c^{Cre}$ mice, suggesting that chase or oral gavage might reconstitute microbes that are deficient in the microbiota of $Tsc1^{f/f}CD11c^{Cre}$ mice.

To identify the microbes whose abundance regulates food intake and body mass in $Tsc1^{f/f}CD11c^{Cre}$ mice, we used 16S rRNA sequencing to follow changes in microbial composition in $Tsc1^{f/f}CD11c^{Cre}$ mice subjected to the microbiome chase experimental paradigm. We found that 3 sequence variants assigned the taxonomic annotations *Lactobacillus johnsonii* group (species), *Rikenellaceae* RC9 group (genus), and *Muribaculaceae* group (family) were significantly different between microbiomes of $Tsc1^{f/f}CD11c^{Cre}$ mice that were transferred into clean cages or $Tsc1^{f/f}$ dirty cages (Figure 3D, 3I). However, *Lactobacillus* was the only clade that was reduced in microbiomes of $Tsc1^{f/f}CD11c^{Cre}$ mice that were housed separately after weaning (Figure 3J and Figure 2F). As multiple species could be mapped to these clades, we performed selective culture of *Lactobacillus* species followed by complete 16S rRNA sequencing of the isolated colonies. Based on the complete 16S rRNA sequence, the sequence variant of *Lactobacillus* that was cultured from stool of $Tsc1^{f/f}$ mice, referred here to as *Lactobacillus* strain Q1-7, taxonomically matched *L. johnsonii* (Figure S3E). This assignment to *L. johnsonii* was based on a 99% nucleotide identity match to *L. johnsonii* CIP 103620 (accession NR_117574.1). Furthermore, we found that the abundance of *L. johnsonii* group but not *Rikenellaceae* or *Muribaculaceae* increased over baseline in $Tsc1^{f/f}CD11c^{Cre}$ mice during the course of the chase experiment and declined when the microbial chase with feces from $Tsc1^{f/f}$ mice was stopped (Figure 3K and Figure S3F, G). These findings suggest that abundance of *Lactobacillus* strain Q1-7 might be causally linked to decreases in food intake and body mass observed in separately housed $Tsc1^{f/f}CD11c^{Cre}$ mice.

Reconstitution of *Lactobacillus* strain Q1-7 increases food intake and body mass in $Tsc1^{f/f}CD11c^{Cre}$ mice

We next asked whether reconstitution of *Lactobacillus* strain Q1-7 into $Tsc1^{f/f}CD11c^{Cre}$ mice can increase food intake and body mass. We found that when $Tsc1^{f/f}CD11c^{Cre}$ mice were gavaged with fecal contents supplemented with *Lactobacillus* strain Q1-7 ($5x10^9$ cfu), body mass and food intake increased progressively over a period of 5 weeks (Figure 4A, B). Quantitative PCR verified increased relative abundance of *Lactobacillus* in microbiota of $Tsc1^{f/f}CD11c^{Cre}$ mice (Figure 4C), indicating that oral introduction of *Lactobacillus* strain Q1-7 is sufficient to increase food intake and body mass in $Tsc1^{f/f}CD11c^{Cre}$ mice. Since previous studies have suggested a role for microbiome-derived short chain fatty acids (butyrate, acetate, and propionate) and metabolites (succinate) in food intake and glucose homeostasis in obese animals (De Vadder et al., 2016; Frost et al., 2014; Koh et al., 2016; Schroeder and Backhed, 2016), we performed targeted metabolomics on cecal, fecal, and plasma samples from $Tsc1^{f/f}$ and $Tsc1^{f/f}CD11c^{Cre}$ mice. Mass spectroscopy and NMR-based metabolomics revealed that levels of short chain fatty acids and other metabolites were largely similar in cecum, feces, and plasma of both groups of mice (Figure 4D and Figure S3H). These findings are consistent with our observations that energy extraction is similar in both genotypes (Figure 1I), suggesting that shifts in abundance of *L. johnsonii* group likely regulate food intake by other unknown mechanisms (Schroeder and Backhed, 2016).

We next asked how mTORC1 signaling in CD11c cells regulates abundance of *Lactobacillus* strain Q1-7 in the gut. To address this question, we began by characterizing intestinal immune cells because they are known to sample luminal contents to regulate intestinal immunity and microbial homeostasis (Ko and Chang, 2015). Using flow cytometry, we found

that numbers of various macrophage and dendritic cell subsets (both $CD11c^{+}$ and $CD11c^{-}$) and B cells were similar in the small intestines and colon of $Tsc1^{f/f}$ and $Tsc1^{f/f}CD11c^{Cre}$ mice (Figure 4E and Figure S4A, B). Consistent with these observations, the numbers of Peyer's patches and intestinal lymphoid structures were also similar between the two genotypes (Figure S4C). These results suggested that activation of mTORC1 signaling in CD11c cells might affect microbial homeostasis by altering their antigen presentation function. In support of this hypothesis, we observed higher mTORC1 activity in lamina propria CD11c cells of $Tsc1^{f/f}CD11c^{Cre}$ mice, which was associated with decreased capacity for antigen presentation *in vitro* (Figure S4D, E), as reported previously (Luo et al., 2017; Wang et al., 2013).

Secretory IgA directed against bacterial antigens has been proposed to shape intestinal microbial composition by multiple mechanisms, including inhibition of bacterial motility, reduction in bacterial fitness, exclusion of immune cells from the inner mucus layer, and creation of a specific mucosal niche to promote stable colonization by specific microbes (Cullender et al., 2013; Donaldson et al., 2018; Gutzeit et al., 2014; Peterson et al., 2007). Because bacterial antigen presentation by lamina propria phagocytes, including CD11c cells, is critical for development of IgA secreting plasma cells, we hypothesized that deletion of Tsc1 in CD11c cells might alter the amount or specificity of secreted IgA against *Lactobacillus* strain Q1-7. We found that while the concentration of free IgA in stool was similar between $Tsc1^{f/f}$ and $Tsc1^{f/f}CD11c^{Cre}$ mice (Figure 4F), the bacterial bound IgA was significantly reduced in stool of 4-week-old $Tsc1^{f/f}CD11c^{Cre}$ mice (Figure 4G). These observations led us to ask whether there was specific reduction in IgA directed against *Lactobacillus* strain Q1-7 in $Tsc1^{f/f}CD11c^{Cre}$ mice. To test this hypothesis, we purified free IgA from stool of $Tsc1^{f/f}$ and $Tsc1^{f/f}CD11c^{Cre}$ mice and performed an *in vitro* binding assay with cultured *Lactobacillus* strain Q1-7. We found that the

stool of Tsc1$^{f/f}$CD11c^{Cre} mice contained less IgA that could specifically bind to *Lactobacillus* strain Q1-7 (Figure 4H), suggesting that reduced production of IgA directed against *Lactobacillus* strain Q1-7 might impair its stable colonization in the gastrointestinal tract of Tsc1$^{f/f}$CD11c^{Cre} mice.

DISCUSSION

Previous studies have highlighted a role for inflammation and microbial dysbiosis in metabolic dysfunction associated with disease states of obesity and insulin resistance (Hotamisligil, 2017; Lee et al., 2018; Maruvada et al., 2017; Schroeder and Backhed, 2016; Sonnenburg and Backhed, 2016). However, the physiologic importance of these systems in maintenance of energy balance in healthy animals is less well understood. The data presented here provide an example of a transkingdom circuit involving CD11c cells and the gut microbe *Lactobacillus* strain Q1-7, which regulates food intake and body weight in lean animals. Utilization of a modified set of Koch's postulates allowed us to identify this transkingdom circuit in Tsc1$^{f/f}$CD11c^{Cre} mice. First, we found that the reduced food intake and body mass in Tsc1$^{f/f}$CD11c^{Cre} mice was dependent on the host microbiome. Second, 16S rRNA sequencing of cohoused and microbiome chased mice led to the identification of *L. johnsonii* group as being selectively depleted in microbiome of Tsc1$^{f/f}$CD11c^{Cre} mice. Third, *Lactobacillus* strain Q1-7 was selectively cultured from the microbiome of Tsc1$^{f/f}$ mice, and its reconstitution into Tsc1$^{f/f}$CD11c^{Cre} mice increased food intake and body mass. And fourth, Tsc1$^{f/f}$CD11c^{Cre} mice produced lower levels of *Lactobacillus* strain Q1-7-specific IgA, which is likely required for the stable colonization *Lactobacillus* strain Q1-7 in its microbial niche.

A major challenge in the microbiome field is to identify specific microbial pathways and products that modulate host physiology and contribute to pathogenesis of disease (Maruvada et

al., 2017; Sonnenburg and Backhed, 2016). Although previous studies have implicated microbiome-derived short chain fatty acids, such as acetate, butyrate, and propionate, in regulation of food intake and weight gain (Frost et al., 2014; Koh et al., 2016), the levels of these and other metabolites were not significantly different between $Tsc1^{f/f}$ and $Tsc1^{f/f}CD11c^{Cre}$ (Figure 4D and S3H). In line with these observations, circulating levels of hormones that regulate satiety and meal size, such as leptin and GLP-1, failed to account for the effects *L. johnsonii* group on feeding behavior (Figure S3A-C). Together, these findings suggest that immune-microbiome interactions might employ distinct mechanisms to maintain metabolic homeostasis in healthy animals, an area that will be worthy of future investigations.

Limitations of Study

There are some limitations of the present study. First, it is well appreciated that the host-microbiome interactions are dynamic and dependent on the host environment. Thus, it remains unknown how environmental stimuli (diet, ambient temperature, and housing facility) might impact the microbial composition and metabolic phenotypes of $Tsc1^{f/f}CD11c^{Cre}$ mice. Second, CD11c is broadly expressed on dendritic cells, which reside at barrier surfaces and in lymphoid tissues. Thus, the precise location and mechanisms by which CD11c cells regulate production of IgA and abundance of *Lactobacillus* strain Q1-7 in the gut remain to be elucidated. Third, while we found that activation of nutrient sensing mTORC1 pathway in CD11c cells regulates food intake and body weight, the mechanisms by which nutrients or microbial products modulate mTORC1 signaling to alter functionality of CD11c cells, specifically those that reside in the lamina propria of the gut, will need to be investigated in the future. And fourth, it remains to be determined whether the transkingdom circuit identified here is representative of a broader mechanism for homeostatic regulation of food intake and body weight in mammals.

ACKNOWLEDGMENTS

We thank members of the Chawla laboratory and A. Loh for comments on the manuscript, A. Savage for assistance with SI and colon flow cytometry, and X. Cui for assistance with mouse husbandry. The authors' work was supported by grants from NIH (DK094641, DK101064, P30DK098722) to A.C. and (C2273232, and HK122593) to P.J.T. Stipend support was provided by NIH NIDDK and UCSF MSTP (F31DK112669 and T32GM007618) to D.N.C. K.G. was supported by a postdoctoral fellowship from Hillblom Fellowship and CVRI T32 grant. Q.Y.A was supported by Agency for Science, Technology and Research, Singapore (National Science Scholarship). J.E.B. was supported by National Science and Engineering Research Council of Canada Postdoctoral Fellowship. The authors declare that they have no competing financial interests.

AUTHOR CONTRIBUTION

D.N.C., Q.Y.A., J.E.B., K.G., and J.C. designed and performed the main experiments. D.N.C., Q.Y.A., J.E.B., K.G., J.C., A.D.T., P.J.T., and A.C. conceived, discussed, interpreted the results, and wrote the paper.

REFERENCES

Belinson, H., Savage, A.K., Fadrosh, D., Kuo, Y.M., Lin, D., Valladares, R., Nusse, Y., Wynshaw-Boris, A., Lynch, S.V., Locksley, R.M., et al. (2016). Dual epithelial and immune cell function of Dvl1 regulates gut microbiota composition and intestinal homeostasis. JCI Insight *1*.

Cai, J., Zhang, L., Jones, R.A., Correll, J.B., Hatzakis, E., Smith, P.B., Gonzalez, F.J., and Patterson, A.D. (2016). Antioxidant Drug Tempol Promotes Functional Metabolic Changes in the Gut Microbiota. J Proteome Res *15*, 563-571.

Callahan, B.J., McMurdie, P.J., Rosen, M.J., Han, A.W., Johnson, A.J., and Holmes, S.P. (2016). DADA2: High-resolution sample inference from Illumina amplicon data. Nature methods *13*, 581-583.

Cannon, B., and Nedergaard, J. (2011). Nonshivering thermogenesis and its adequate measurement in metabolic studies. The Journal of experimental biology *214*, 242-253.

Caporaso, J.G., Lauber, C.L., Walters, W.A., Berg-Lyons, D., Huntley, J., Fierer, N., Owens, S.M., Betley, J., Fraser, L., Bauer, M., et al. (2012). Ultra-high-throughput microbial community analysis on the Illumina HiSeq and MiSeq platforms. ISME J *6*, 1621-1624.

Cullender, T.C., Chassaing, B., Janzon, A., Kumar, K., Muller, C.E., Werner, J.J., Angenent, L.T., Bell, M.E., Hay, A.G., Peterson, D.A., et al. (2013). Innate and adaptive immunity interact to quench microbiome flagellar motility in the gut. Cell Host Microbe *14*, 571-581.

De Vadder, F., Kovatcheva-Datchary, P., Zitoun, C., Duchampt, A., Backhed, F., and Mithieux, G. (2016). Microbiota-Produced Succinate Improves Glucose Homeostasis via Intestinal Gluconeogenesis. Cell Metab *24*, 151-157.

Donaldson, G.P., Ladinsky, M.S., Yu, K.B., Sanders, J.G., Yoo, B.B., Chou, W.C., Conner, M.E., Earl, A.M., Knight, R., Bjorkman, P.J., et al. (2018). Gut microbiota utilize immunoglobulin A for mucosal colonization. Science *360*, 795-800.

Dong, F.C., Zhang, L.L., Hao, F.H., Tang, H.R., and Wang, Y.L. (2013). Systemic Responses of Mice to Dextran Sulfate Sodium-Induced Acute Ulcerative Colitis Using H-1 NMR Spectroscopy. Journal of Proteome Research *12*, 2958-2966.

Frost, G., Sleeth, M.L., Sahuri-Arisoylu, M., Lizarbe, B., Cerdan, S., Brody, L., Anastasovska, J., Ghourab, S., Hankir, M., Zhang, S., et al. (2014). The short-chain fatty acid acetate reduces appetite via a central homeostatic mechanism. Nature communications *5*, 3611.

Ganeshan, K., and Chawla, A. (2017). Warming the mouse to model human diseases. Nature reviews. Endocrinology *13*, 458-465.

Gonzalez, A., and Hall, M.N. (2017). Nutrient sensing and TOR signaling in yeast and mammals. The EMBO journal *36*, 397-408.

Gordon, C.J. (2017). The mouse thermoregulatory system: Its impact on translating biomedical data to humans. Physiol Behav *179*, 55-66.

Gutzeit, C., Magri, G., and Cerutti, A. (2014). Intestinal IgA production and its role in host-microbe interaction. Immunological reviews *260*, 76-85.

Heiss, C.N., and Olofsson, L.E. (2018). Gut Microbiota-Dependent Modulation of Energy Metabolism. J Innate Immun *10*, 163-171.

Hotamisligil, G.S. (2017). Inflammation, metaflammation and immunometabolic disorders. Nature *542*, 177-185.

Ko, H.J., and Chang, S.Y. (2015). Regulation of intestinal immune system by dendritic cells. Immune Netw *15*, 1-8.

Koh, A., De Vadder, F., Kovatcheva-Datchary, P., and Backhed, F. (2016). From Dietary Fiber to Host Physiology: Short-Chain Fatty Acids as Key Bacterial Metabolites. Cell *165*, 1332-1345.

Lee, Y.S., Wollam, J., and Olefsky, J.M. (2018). An Integrated View of Immunometabolism. Cell *172*, 22-40.

Ley, R.E., Backhed, F., Turnbaugh, P., Lozupone, C.A., Knight, R.D., and Gordon, J.I. (2005). Obesity alters gut microbial ecology. Proc Natl Acad Sci U S A *102*, 11070-11075.

Lumeng, C.N., Bodzin, J.L., and Saltiel, A.R. (2007). Obesity induces a phenotypic switch in adipose tissue macrophage polarization. J Clin Invest *117*, 175-184.

Luo, Y., Li, W., Yu, G., Yu, J., Han, L., Xue, T., Sun, Z., Chen, S., Fang, C., Zhao, C., et al. (2017). Tsc1 expression by dendritic cells is required to preserve T-cell homeostasis and response. Cell Death Dis *8*, e2553.

Man, K., Kutyavin, V.I., and Chawla, A. (2017). Tissue Immunometabolism: Development, Physiology, and Pathobiology. Cell Metab *25*, 11-26.

Maruvada, P., Leone, V., Kaplan, L.M., and Chang, E.B. (2017). The Human Microbiome and Obesity: Moving beyond Associations. Cell Host Microbe *22*, 589-599.

Moor, K., Fadlallah, J., Toska, A., Sterlin, D., Balmer, M.L., Macpherson, A.J., Gorochov, G., Larsen, M., and Slack, E. (2016). Analysis of bacterial-surface-specific antibodies in body fluids using bacterial flow cytometry. Nature protocols *11*, 1531-1553.

Morton, G.J., Meek, T.H., and Schwartz, M.W. (2014). Neurobiology of food intake in health and disease. Nat Rev Neurosci *15*, 367-378.

Nicholson, J.K., Holmes, E., Kinross, J., Burcelin, R., Gibson, G., Jia, W., and Pettersson, S. (2012). Host-gut microbiota metabolic interactions. Science *336*, 1262-1267.

Patsouris, D., Li, P.P., Thapar, D., Chapman, J., Olefsky, J.M., and Neels, J.G. (2008). Ablation of CD11c-positive cells normalizes insulin sensitivity in obese insulin resistant animals. Cell Metab *8*, 301-309.

Peterson, D.A., McNulty, N.P., Guruge, J.L., and Gordon, J.I. (2007). IgA response to symbiotic bacteria as a mediator of gut homeostasis. Cell Host Microbe *2*, 328-339.

Saxton, R.A., and Sabatini, D.M. (2017). mTOR Signaling in Growth, Metabolism, and Disease. Cell *168*, 960-976.

Schroeder, B.O., and Backhed, F. (2016). Signals from the gut microbiota to distant organs in physiology and disease. Nat Med *22*, 1079-1089.

Shi, X., Xiao, C., Wang, Y., and Tang, H. (2013). Gallic Acid Intake Induces Alterations to Systems Metabolism in Rats. Journal of Proteome Research *12*, 991-1006.

Silverman, J.D., Washburne, A.D., Mukherjee, S., and David, L.A. (2017). A phylogenetic transform enhances analysis of compositional microbiota data. Elife *6*.

Sonnenburg, J.L., and Backhed, F. (2016). Diet-microbiota interactions as moderators of human metabolism. Nature *535*, 56-64.

Stappenbeck, T.S., and Virgin, H.W. (2016). Accounting for reciprocal host-microbiome interactions in experimental science. Nature *534*, 191-199.

Tian, X.Y., Ganeshan, K., Hong, C., Nguyen, K.D., Qiu, Y., Kim, J., Tangirala, R.K., Tontonoz, P., and Chawla, A. (2016). Thermoneutral Housing Accelerates Metabolic Inflammation to Potentiate Atherosclerosis but Not Insulin Resistance. Cell Metab *23*, 165-178.

Tian, Y., Zhang, L.M., Wang, Y.L., and Tang, H.R. (2012). Age-Related Topographical Metabolic Signatures for the Rat Gastrointestinal Contents. Journal of Proteome Research *11*, 1397-1411.

Turnbaugh, P.J., Hamady, M., Yatsunenko, T., Cantarel, B.L., Duncan, A., Ley, R.E., Sogin, M.L., Jones, W.J., Roe, B.A., Affourtit, J.P., et al. (2009). A core gut microbiome in obese and lean twins. Nature *457*, 480-484.

Turnbaugh, P.J., Ley, R.E., Mahowald, M.A., Magrini, V., Mardis, E.R., and Gordon, J.I. (2006). An obesity-associated gut microbiome with increased capacity for energy harvest. Nature *444*, 1027-1031.

Valdearcos, M., Douglass, J.D., Robblee, M.M., Dorfman, M.D., Stifler, D.R., Bennett, M.L., Gerritse, I., Fasnacht, R., Barres, B.A., Thaler, J.P., et al. (2017). Microglial Inflammatory Signaling Orchestrates the Hypothalamic Immune Response to Dietary Excess and Mediates Obesity Susceptibility. Cell Metab *26*, 185-197 e183.

Wang, Q., Garrity, G.M., Tiedje, J.M., and Cole, J.R. (2007). Naive Bayesian classifier for rapid assignment of rRNA sequences into the new bacterial taxonomy. Appl Environ Microbiol *73*, 5261-5267.

Wang, Y., Huang, G., Zeng, H., Yang, K., Lamb, R.F., and Chi, H. (2013). Tuberous sclerosis 1 (Tsc1)-dependent metabolic checkpoint controls development of dendritic cells. Proc Natl Acad Sci U S A *110*, E4894-4903.

Waterson, M.J., and Horvath, T.L. (2015). Neuronal Regulation of Energy Homeostasis: Beyond the Hypothalamus and Feeding. Cell Metab *22*, 962-970.

Zheng, X., Qiu, Y., Zhong, W., Baxter, S., Su, M., Li, Q., Xie, G., Ore, B.M., Qiao, S., Spencer, M.D., et al. (2013). A targeted metabolomic protocol for short-chain fatty acids and branched-chain amino acids. Metabolomics : Official journal of the Metabolomic Society *9*, 818-827.

FIGURE LEGENDS

Figure 2.1. Activation of mTORC1 signaling in CD11c cells reduces body mass and food intake.
(A) Body mass of $Tsc1^{f/f}$ and $Tsc1^{f/f}CD11c^{Cre}$ mice fed high fat diet (HFD) from age of 6 to 19 weeks (n=6-8 per genotype; analyzed by two-way ANOVA). (B, C) Glucose (B) and insulin (C) tolerance tests of $Tsc1^{f/f}$ and $Tsc1^{f/f}CD11c^{Cre}$ mice fed HFD (n=4-5 per genotype; analyzed by two-way ANOVA). (D) Body mass of $Tsc1^{f/f}$ and $Tsc1^{f/f}CD11c^{Cre}$ mice fed low-fat regular chow diet (n=5 per genotype; analyzed by two-way ANOVA). (E) Body composition analysis by DEXA of $Tsc1^{f/f}$ and $Tsc1^{f/f}CD11c^{Cre}$ mice fed low-fat regular chow diet (n=5 per genotype; analyzed by t-test). (F-H) Oxygen consumption (F), total activity (G), and food consumption over 24 hours in 8-week-old $Tsc1^{f/f}$ and $Tsc1^{f/f}CD11c^{Cre}$ mice (n=7-9 per genotype; analyzed by t-test). (I) Assessment of energy harvest in 8-week-old $Tsc1^{f/f}$ and $Tsc1^{f/f}CD11c^{Cre}$ mice fed low-fat regular chow diet using fecal bomb calorimetry (n=8-9 per genotype; analyzed by t-test). (J) Plasma concentrations of inflammatory cytokines in 8-week-old $Tsc1^{f/f}$ and $Tsc1^{f/f}CD11c^{Cre}$ mice fed low-fat regular chow diet (n=4 per genotype; analyzed by t-test). (K) Flow cytometric analysis of microglial populations in hypothalami of $Tsc1^{f/f}$ and $Tsc1^{f/f}CD11c^{Cre}$ mice fed low-fat regular chow diet. Total microglia ($CD45^{mid}CX3CR1^{+}$); $CD11c^{+}$ microglia ($CD45^{mid}CX3CR1^{+}CD11c^{+}$) and activated microglia ($CD45^{mid}CX3CR1^{+}CD68^{+}$), (n= 5 per genotype; analyzed by t-test). Dashed line designates that $CD11c^{+}$ and activated microglia are subsets of total microglia. Data are presented as mean ± SEM.

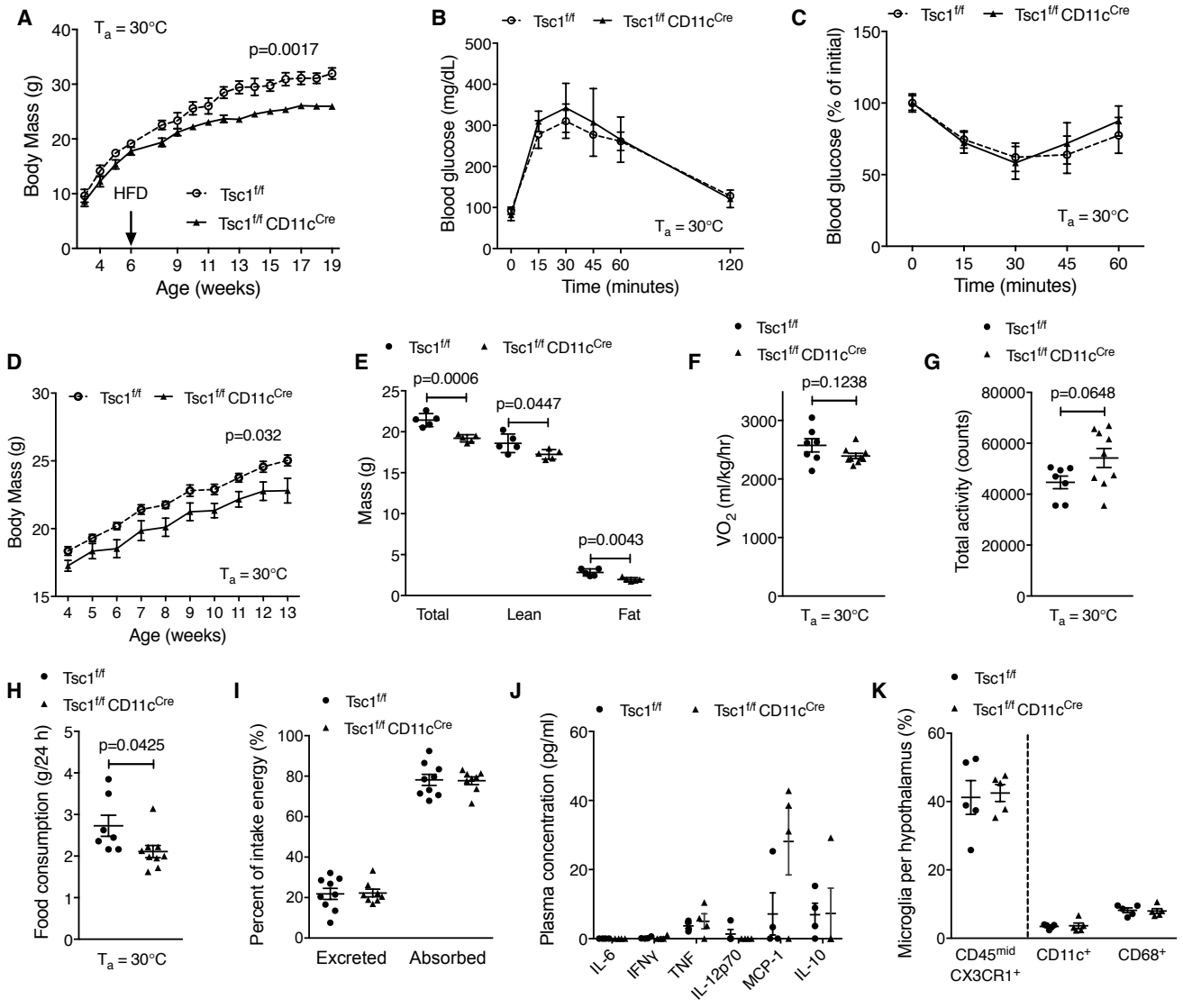

Figure 2.1. Activation of mTORC1 signaling in CD11c cells reduces body mass and food intake.

Figure 2.2. Microbiome of $Tsc1^{f/f}CD11c^{Cre}$ mice reduces food intake and body mass.
(A) Body mass of $Tsc1^{f/f}$ and $Tsc1^{f/f}CD11c^{Cre}$ mice on low-fat regular chow diet (n=5-15 per genotype; analyzed by t-test). (B-D) Body mass (B), body composition (C), and food consumption (D) in $Tsc1^{f/f}$ and $Tsc1^{f/f}CD11c^{Cre}$ mice fed low-fat regular chow diet and cohoused after weaning (n=4 per genotype; analyzed by two-way ANOVA (B) and t-test (C, D)). (E) PCoA using Bray Curtis dissimilarity for ordination of microbial communities of $Tsc1^{f/f}$ and $Tsc1^{f/f}CD11c^{Cre}$ mice fed low-fat regular chow diet that were cohoused or housed separately after weaning. Each data point represents a single mouse at 8 weeks of age, (n=7-8 per genotype; analyzed by ADONIS p=0.002, R2=0.472 comparing separately-housed $Tsc1^{f/f}CD11c^{Cre}$ mice to separately-housed $Tsc1^{f/f}$ mice and cohoused mice). (F) Phylogenetic tree of 16S rRNA sequence variants and internal nodes that are significantly different between $Tsc1^{f/f}$ and $Tsc1^{f/f}CD11c^{Cre}$ mice housed separately. Black circles denote significantly different nodes analyzed by Welch's *t* test with multiple testing correction (FDR<0.1) with the size of the node representing absolute fold change. Colored tips denote significantly different sequence variants analyzed by DESeq2 (FDR<0.1) with color representing fold change comparing $Tsc1^{f/f}CD11c^{Cre}$ mice to $Tsc1^{f/f}$ mice. Bacterial clades of interest are highlighted in grey. (G, H) Change in body mass (G) and food consumption (H) in C57BL/6J mice after 8 weeks of oral gavage of fecal contents from $Tsc1^{f/f}CD11c^{Cre}$ or $Tsc1^{f/f}$ mice (n=7 per genotype; analyzed by t-test). Data are presented as mean ± SEM.

Figure 2.2. Microbiome of Tsc1$^{f/f}$CD11c^{Cre} mice reduces food intake and body mass.

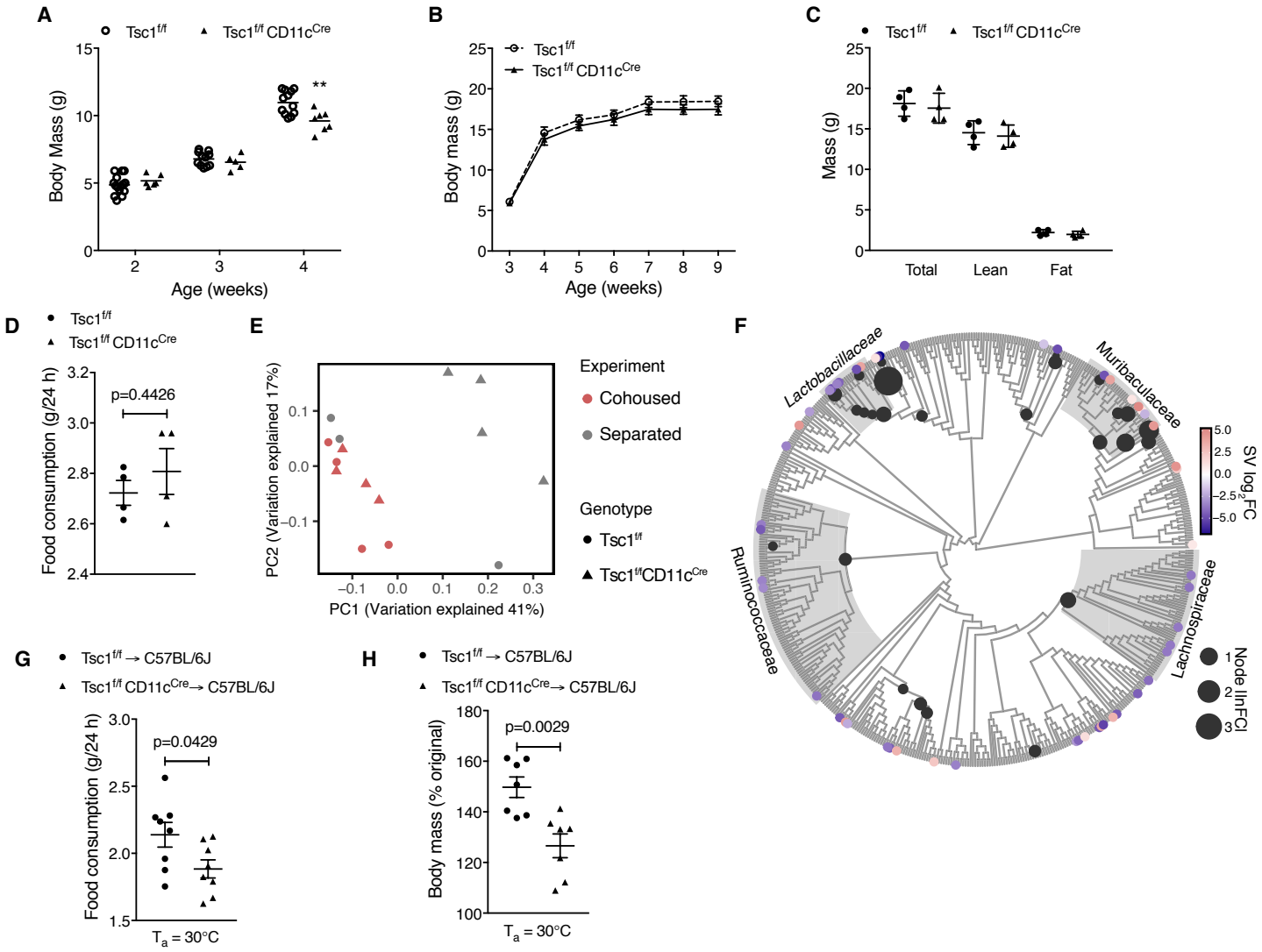

Figure 2.3. Abundance of *Lactobacillus johnsonii* is reduced in microbiota of $Tsc1^{f/f}CD11c^{Cre}$ mice.
(A) Schematic of $Tsc1^{f/f}$ mice being chased by microbiome of $Tsc1^{f/f}CD11c^{Cre}$ mice. (B, C) Change in body mass (B) and food intake (C) of $Tsc1^{f/f}$ mice during chase with microbiome of $Tsc1^{f/f}CD11c^{Cre}$ mice, (n=4-5, analyzed by 2-way ANOVA with Sidak's multiple comparisons test (B) and t-test (C)). (D) Schematic of $Tsc1^{f/f}CD11c^{Cre}$ mice being chased by microbiome of $Tsc1^{f/f}$ mice. (E, F) Change in body mass (E) and food consumption (F) in $Tsc1^{f/f}CD11c^{Cre}$ mice during chase with microbiome of $Tsc1^{f/f}$ mice, (n=4-5, analyzed by 2-way ANOVA with Sidak's multiple comparisons test (E) and t-test (F)). (G, H) Change in body mass (G) and food consumption (H) after 8 weeks of oral gavage of fecal contents from $Tsc1^{f/f}CD11c^{Cre}$ or $Tsc1^{f/f}$ mice into $Tsc1^{f/f}CD11c^{Cre}$ mice (n=8-9 per genotype; analyzed by t-test). (I) Volcano plot of 16S rRNA sequence variants that were different between $Tsc1^{f/f}CD11c^{Cre}$ moved to clean cage or chased with microbiome of $Tsc1^{f/f}$ mice. Red dots represent statistically significant sequence variants (analyzed by linear mixed effects model; log2 fold change>1 and FDR<0.1). Full taxonomic annotations for the three significant sequence variants are: *Lactobacillus johnsonii*/crispatus/gasseri/helveticus/hominis/iatae/johnsonii/kefiranofaciens/prophage/taiwanensis (species), *Rikenellaceae* RC9 gut group (genus), and Muribaculaceae (family). (J) Schematic of the flowchart used to identify *L. johnsonii* as being less abundant in microbiome of $Tsc1^{f/f}CD11c^{Cre}$ mice. (K) Changes in relative abundance of *L. johnsonii* in stool of $Tsc1^{f/f}CD11c^{Cre}$ mice during chase with microbiome of $Tsc1^{f/f}$ mice (as in E, F). The dashed lines denote the period of microbiome chase experiment, (n = 2 per chase group; error bars represent range; analyzed by linear mixed effects model FDR<0.1). Data are presented as mean ± SEM.

Figure 2.3. Abundance of *Lactobacillus johnsonii* is reduced in microbiota of Tsc1$^{f/f}$CD11c^{Cre} mice.

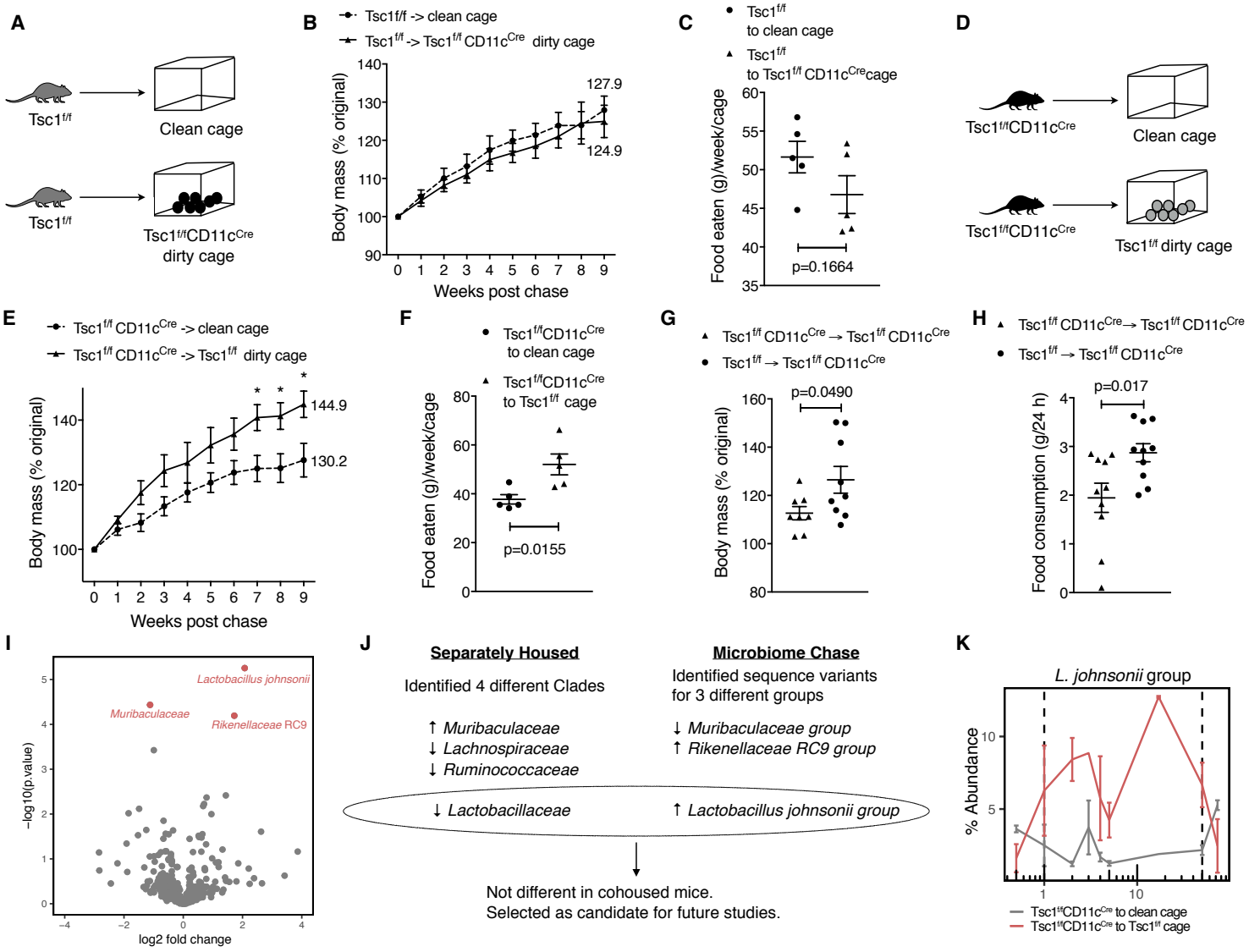

Figure 2.4. Reconstitution of *Lactobacillus* strain Q1-7 increases food intake and body mass in $Tsc1^{f/f}CD11c^{Cre}$ mice.
(A-C) Change in body mass (A), food intake (B), and qRT-PCR analysis for relative abundance of *Lactobacillus* relative in feces (C) of $Tsc1^{f/f}CD11c^{Cre}$ mice orally gavaged with fecal contents of $Tsc1^{f/f}CD11c^{Cre}$ mice that were supplemented with vehicle or *Lactobacillus* strain Q1-7 ($5x10^9$ cfu) for 6 weeks, (n=6-7 per genotype; analyzed by t-test). (D) Quantification of cecal, fecal, and plasma short chain fatty acids by GC-MS (n=7 per genotype; analyzed by Mann-Whitney). (E) Quantification by flow cytometry of B cells and IgA^+ B cells in proximal small intestines (SI) and colons of 8-week-old $Tsc1^{f/f}$ and $Tsc1^{f/f}CD11c^{Cre}$ mice (n=3-4 per genotype; analyzed by t-test). (F, G) Quantification of free IgA (F) and bacterial bound IgA (G) in stool of 4-week-old $Tsc1^{f/f}$ and $Tsc1^{f/f}CD11c^{Cre}$ mice (n=9-11 per genotype; analyzed by t-test). (H) Quantification of free IgA specific for *Lactobacillus* strain Q1-7 in stool of 4-week-old $Tsc1^{f/f}$ and $Tsc1^{f/f}CD11c^{Cre}$ mice (n=9-11 per genotype; analyzed by t-test). Data are presented as mean ± SEM.

Figure 2.4. Reconstitution of *Lactobacillus* strain Q1-7 increases food intake and body mass in Tsc1$^{f/f}$CD11c^{Cre} mice.

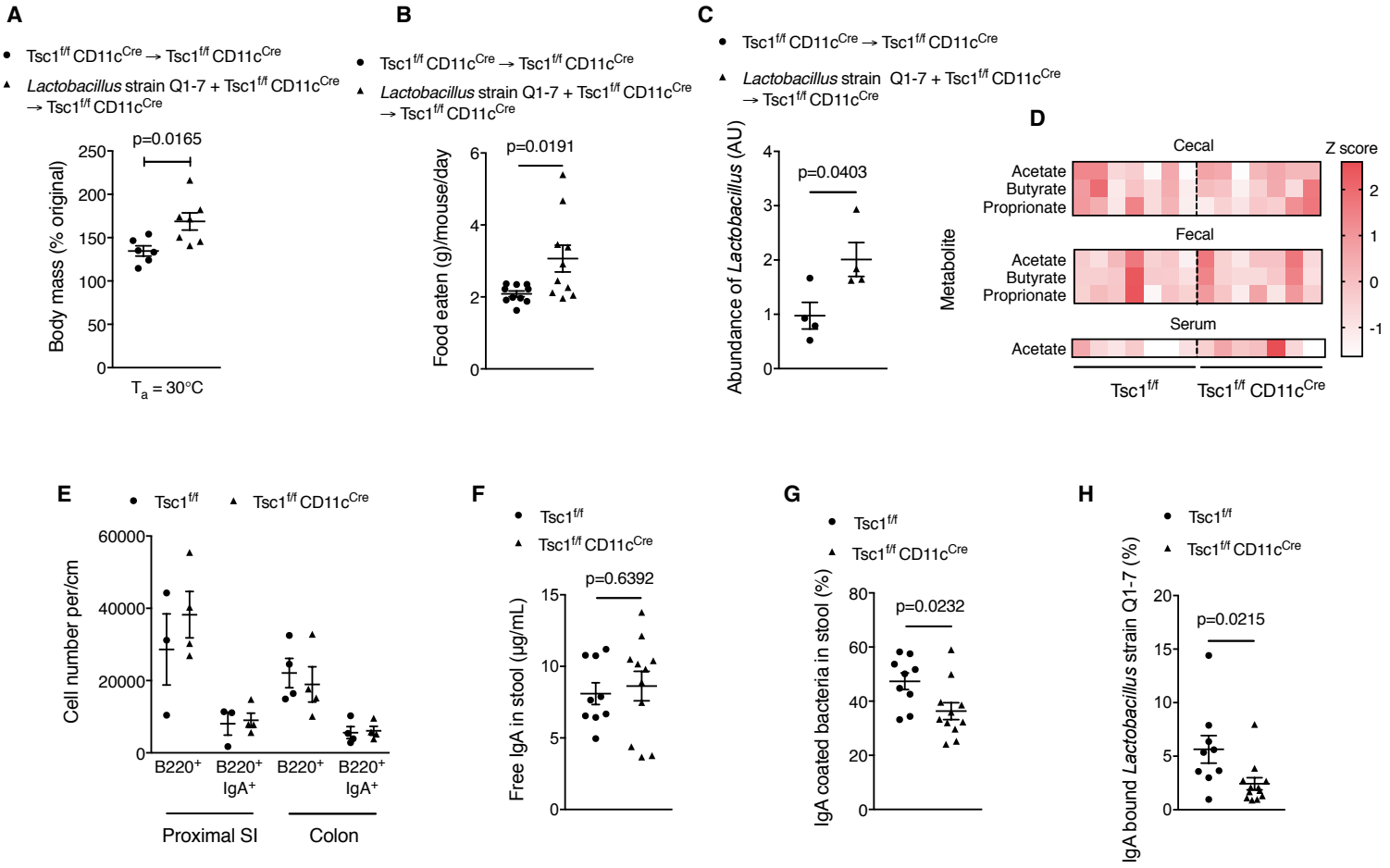

METHODS

Animal studies

All animal studies were conducted under an approved Institutional Animal Care and Use Committee (IACUC) protocol at University of California, San Francisco (UCSF). Mice were housed at 30°C after weaning (unless otherwise indicated) in Darwin or Power Scientific environmental chambers under a 12-hr light:dark cycle. $Tsc1^{f/f}$ and $CD11c^{Cre}$ mice were purchased from Jackson Laboratories, backcrossed onto C57BL/6J background (*Nnt* null) for 10 generations, and used to generate $Tsc1^{f/f}$ $CD11c^{Cre}$ mice. Littermate $Tsc1^{f/f}$ and $Tsc1^{f/f}CD11c^{Cre}$ mice were either separated at weaning or continually cohoused for the duration of the experiments. Mice were fed normal chow diet (5053, Pico labs) or high fat diet (D12492i, Research Diets). For microbiome chase experiments, mice were moved to a clean cage or a dirty cage every day for duration of the experiment.

Food intake

Successive food consumption was calculated using the formula: [(Food mass) on Day(N) – (Food mass) on Day(N+1)], and values were adjusted for the number of mice per cage. The same number of mice per cage were compared between experimental groups to minimize the impact of housing density on food consumption.

Energy expenditure and body composition analysis

Body composition (fat and lean mass) analysis were performed on anesthetized mice using Dual-energy X-ray absorptiometry (DEXA). For measurement of energy expenditure, food intake, and locomotor activity, mice were placed in CLAMS (Columbus Instruments) cages that housed in an environmental chamber set at 30°C. After acclimatization for one day, data on oxygen consumption, locomotor activity, and food intake was collected every 22 minutes.

Glucose and insulin tolerance tests

For glucose and insulin tolerance tests, mice were intraperitoneally injected with glucose (1.5g/kg of body weight) after 14h fast or insulin (1U/kg of body weight) after 6h fast, and blood glucose was measured at regular intervals using tail blood.

Bomb calorimetry

Fecal samples were collected and lyophilized to obtain dried mass. Approximately, 200 mg of dried stool was pressed into a pellet using a pellet press. Gross energy content was measured using a semimicro oxygen bomb in an isoperibol calorimeter. The calorimeter energy equivalent factor was determined using benzoic acid standards. Data are presented as a percentage of energy consumed by each genotype.

Quantitative RT-PCR

As per manufacturer's protocols, fecal DNA or tissue RNA was extracted using Bioline Fecal DNA or RNA kits, respectively. RNA was reverse transcribed into cDNA using qScript cDNA Supermix (Quanta), and quantitative PCR was performed on CFX384 real-time PCR detection system (Bio-rad). Relative expression levels were determined using the ΔΔCt method with 36B4 or GAPDH serving as an internal reference. *Lactobacillus* expression was normalized to stool weight. Primers used are listed in Supplemental Table 1.

Histology

Brown fat, small intestines, and colons were fixed in 10% formalin for 4-24 hours and stored at 4°C in 20% sucrose in PBS. Paraffin embedded tissues were sectioned at 5 μm, stained with hematoxylin and eosin, and imaged using an Olympus BX41 equipped with a Digital Sight DS-Fi1 camera (Nikon).

Immunoblotting

Snap-frozen tissues were homogenized in modified RIPA buffer (420 mM NaCl, 1% NP- 40, 0.1% SDS, 0.5% sodium deoxycholate, 50 mM Tris pH 7.5, and protease inhibitor cocktail) using a TissueLyser II (Qiagen). Total protein was separated by SDS-PAGE, transferred to nitrocellulose membranes, and probed with primary anti-UCP1 and secondary anti-IgG HRP antibodies. Immunoblotted proteins were detected using SuperSignal West Pico Chemiluminescent Substrate (Thermo Scientific).

Bone marrow dendritic cells (BMDCs) and antigen presentation assay

Bone marrow cells were flushed from femurs and tibias of $Tsc1^{f/f}$ and $Tsc1^{f/f}CD11c^{Cre}$ mice, and cultured in RPMI 1640 supplemented with 10% FBS, 10 mM HEPES pH 7.0, 100 U/ml penicillin, 1000 U/ml streptomycin, 20 mM l-glutamine, and 20 ng/ml GM-CSF. On day 3 of culture, half the medium was replaced with fresh medium. On day 7, BMDCs were used for experiments or flow cytometric analysis. For in vitro antigen presentation assay, BMDCs from $Tsc1^{f/f}$ and $Tsc1^{f/f}CD11c^{Cre}$ mice were pulsed with OVA 323-339 (10μg/ml) or 257-264 (25μg/ml) for 4 hours. CD4 and CD8 T cells were purified from the spleens of OT-II/OT-I transgenic mice using MACS kits. T cells were pulsed with CFSE (2 μM) for 5 min at 37 °C and then washed twice with PBS. Purified T cells ($1x10^5$) were then incubated with OVA BMDCs ($1x10^5$) for 3 days. Cells were washed, and stained with antibodies against CD4, CD8 and CD69 (marker of T cell activation). Data was acquired using FACSVerse (Becton Dickinson) and analyzed using FlowJo software.

Flow cytometry and serum cytokines

Small intestine and colon flow cytometric analyses were performed as described previously (Belinson et al., 2016). Briefly, proximal and distal intestine and colon were dissected. Colon

length was measured and numbers of Peyer's Patches (PPs) and intestinal lymphoid structures (ILSs) were removed and counted. The gut tissue was then shaken in three times in 20 ml cold PBS, washed twice for 20 minutes at 37°C in 20 ml of Ca^{2+}/Mg^{2+}-free HBSS containing 5 mM DTT, 5 mM EDTA, 10 mM HEPES, and 2% FCS, followed by washing in 20 ml of Ca^{2+}/Mg^{2+}-replete HBSS containing 10 mM HEPES with 2% FCS. Tissues were then digested for 30 minutes at 37°C in 5 ml of Ca^{2+}/Mg^{2+}-replete HBSS containing 10 mM HEPES, 2% FCS, 30 μg/ml DNase, 0.1 Wünsch/ml LibTM (Roche), homogenized in C tubes using a gentleMACS tissue dissociator (Miltenyi), and then passed through a 100-μm filter. The filtrate was separated in a 40%/90% Percoll gradient and stained for innate and adaptive immune cells. Data was acquired using FACSVerse (Becton Dickinson) and analyzed using FlowJo software. Plasma cytokine levels were measured by cytometric bead array-mouse inflammation kit (BD Biosciences, San Jose, CA) as per manufacturer's instructions.

Intestinal macromolecular permeability assay

Intestinal macromolecular permeability assay was performed in mice after a 5h fast. Mice were orally gavaged with 400μg of fluorescein isothiocyanate (FITC)-dextran (4kDA/g body weight), and 5 hours later, FITC-dextran was detected in plasma samples using flow cytometry.

Measurement of GLP-1 and leptin

For measurement of active GLP-1, mice were fasted for 6 hours and given 2g/kg glucose by oral gavage. 15 mins later, mice were bled retro-orbitally using ice-cooled heparinized capillary tubes. DPP4 inhibitor was immediately added at 10μL per ml of blood. Samples were centrifuged at 1,000g for 10 mins and GLP-1 levels measured according to manufacturer's protocol. For measurement of leptin, mice were bled retro-orbitally at 7am, blood was centrifuged at 8,000g for

8 mins. Resulting plasma was diluted 5x with PBS and leptin levels measured according to manufacturer's instructions.

Short chain fatty acids quantitation by GC-MS

Short chain fatty acids were quantified with a previously described propyl esterification method using Agilent 7890A gas chromatograph coupled with Agilent 5975 mass spectrometer (Agilent Technologies Santa Clara, CA). Briefly, 50 mg cecal/fecal samples or 300 µL of serum collected were mixed with 1 mL of 5 mM NaOH containing 10 µg/mL internal standard hexanoic acid-6,6,6-d3 (C/D/N Isotopes Inc, Pointe-Claire, Quebec, Canada), homogenized (Bertin Technologies, Rockville, MD) at 6500 rpm for 1 minute until thoroughly homogenized. 1.0 mm diameter Zirconia/Silica beads (BioSpec, Bartlesville, OK) were added for through homogenization (Zheng et al., 2013). The homogenized samples then were centrifuged (Eppendorf, Hamburg, Germany) at 13,200 x g, 4 °C, 20 minutes. The supernatant was taken and mixed with an aliquot of 500 µL of 1-propanol/pyridine (v/v=3:2) solvent. 100 µL of derivatization reagent propyl chloroformate was added slowly following a brief vortex for 1 minute. Samples were derivatized in an incubator (Thermo Scientific, Marietta OH) at 60 ℃ for an hour. The derivatized samples were extracted with a two-step hexane extraction (300 µL + 200 µL). A total 500 µL of upper layer was transferred to a glass auto sampler vials for GC-MS analysis. A calibration curve with pure standards was drafted for quantitation as described (Cai et al., 2016).

^{1}H NMR-based global metabolomics

Cecal content, feces and serum metabolites were extracted as previously described (Cai et al., 2016; Shi et al., 2013). ^{1}H NMR spectra were recorded at 298 K on a Bruker Avance III 600 MHz spectrometer equipped with an inverse cryogenic probe (Bruker Biospin, Germany). NMR spectra of cecal and fecal samples were acquired using the first increment of NOESY pulse sequence with presaturation (Bruker 1D noesygppr1d pulse sequence). The serum spectra were acquired with a Carr-Purcell-Meiboom-Gill pulse sequence [recycle delay-90°-$(\tau$-180°-$\tau)_n$-acquisition]. Quality of all spectra were improved by phase adjustment, baseline correction and calibration using Topspin 3.0 (Bruker Biospin, Germany). The

spectral region δ 0.50-9.50 was integrated into bins with equal width of 0.004 ppm (2.4 HZ) using AMIX package (V3.8, Bruker Biospin) for relative concentration analysis. The metabolites were assigned based on published results (Cai et al., 2016; Dong et al., 2013; Tian et al., 2012).

IgA Binding Assay

IgA was isolated by homogenizing stool in PBS containing protease inhibitor (0.1 mg/µl) followed by centrifugation at 400g. Supernatant was collected by filtration through a 70 µm strainer followed by centrifugation at 8000g to pellet the bacteria. IgA concentration in the supernatant was quantified by Mouse IgA ELISA (Bethyl Laboratories). For quantifying IgA bound bacteria, bacterial pellets were resuspended in PBS supplemented with 5% goat serum and SYTO BC (ThermoFisher Technologies) followed by incubation for 15 minutes on ice. Anti-IgA-Alexa Fluor 647 (Southern Biotech) was added for 20 minutes on ice. Samples were washed and resuspended in PBS with DAPI (ThermoFisher Technologies) for flow cytometric analysis. Data was acquired on FACSVerse (Becton Dickinson) using a low FSC and SSC threshold (in log scale) to allow for bacterial detection and analyzed using FlowJo software. Samples were gated as $FSC^{+}SSC^{+}SYTOBC^{+}DAPI^{-}$ and assessed for IgA staining. IgA-*Lactobacillus* strain Q1-7 binding assay was performed as previously described (Moor et al., 2016). Briefly, 25µl of $5x10^{6}$cfu/ml *Lactobacillus* strain Q1-7 was incubated with 25µl of free IgA (3µg/ml), which was obtained from stool of $Tsc1^{f/f}$ and $Tsc1^{f/f}CD11c^{Cre}$ mice, in a V-bottom-96 well plate overnight at 4°C. The incubated samples were washed in bacterial flow cytometry buffer (PBS with 2% BSA (wt/vol) and 0.02% sodium azide (wt/vol) by centrifugation at 4,000g for 10min at 4°C. The samples were then stained with 50µl of 10µg/ml IgA-FITC antibody (BD Biosciences) at RT for 15min, washed, and bacterial pellets were resuspended in 300µl bacterial flow cytometry buffer. Data was acquired using FACSVerse (Becton Dickinson) with a low FSC and SSC threshold to

allow bacterial detection and analyzed using FlowJo software. FSC and SSC were set to log scale and gated bacteria were assessed for IgA binding.

16S rRNA Gene Sequencing and Analysis

Mouse fecal pellets were homogenized with bead beating for 5 min (Mini-Beadbeater-96, BioSpec) using beads of mixed size and material (Lysing Matrix E 2mL Tube, MP Biomedicals) in the digestion solution and lysis buffer of a Wizard SV 96 Genome DNA kit (Promega). The samples were then centrifuged for 10 min at 16,000g and the supernatant was transferred to the binding plate. The DNA was then purified according to the manufacturer's instructions. 16S rRNA gene PCR was carried out using GoLay-barcoded 515F/806R primers (Caporaso et al., 2012). 2µL of DNA was combined with 25 µL of AmpliTaq Gold 360 Master Mix (Fisher Scientific), 5 µL of primers (2µM each GoLay-barcoded 515/806R), and 18µL H_2O. Amplification was as follows: 10 min 95˚C, 30x (30s 95˚C, 30s 50˚C, 30s 72˚C), and 7 min 72˚C. Amplicons were quantified with PicoGreen (Quant-It dsDNA; Life Technologies) and pooled at equimolar concentrations. Aliquots of the pools were then column (MinElute PCR Purification Kit; Qiagen) and gel purified (QIAquick Gel Extraction Kit; Qiagen). Libraries were then quantified (KAPA Library Quantifcation Kit; Illumina) and sequenced with a 600 cycle MiSeq Reagent Kit (251x151; Illumina) with 20-50% PhiX. Raw data was deposited in the NCBI Sequence read archive under SRP154475. Reads were demultiplexed using QIIME v1.9.1 (split_libraries_fastq.py) before denoising and processing with DADA2 v1.1.5 under MRO v3.2.5 (Callahan et al., 2016). Taxonomy was assigned using the DADA2 implementation of the RDP classifier using the DADA2 formatted training sets for SILVA123 (benjjneb.github.io/dada2/assign.html) (Wang et al., 2007). A phylogenetic tree was constructed using MUSCLE v3.8.31 using the FastTree algorithm with midpoint rooting. Sequence variants

were filtered such that they were present in more than one sample with at least a total of 10 reads. Diversity metrics were generated using Vegan v2.5-2 with principal coordinate analysis (PCoA) carried out with Ape v5.1. The Wald test in DESeq2 package (v1.20) was used to analyze differential abundances on count data. PhILR transformation was carried out with the package philr v1.6 as described and analyzed using *t test* with multiple testing correction across features/nodes tested (Silverman et al., 2017). For the separated housing experiments, significant nodes and sequence variants were visualized on a phylogenetic tree using the ggtree package v1.12. For the microbiome chase experiment, variance stabilizing transformation (DESeq2 package v1.20) was applied on count data, and time-course analysis was carried out using linear mixed effect models (lmerTest v3.0-1) with mouse as a random effect to account for repeated sampling across time using the with a 0.05 Benjamini-Hochberg false discovery rate cutoff for significance.

Isolation and identification of *Lactobacillus* species

Lactobacillus species were isolated from stool of $Tsc1^{f/f}$ mice by plating diluted stool on MRS agar with and without vancomycin (50μg/mL) followed by incubation at 37°C for 24 hours under anaerobic conditions using BBLTM GasPak 100TM EZ gas generating container (Becton Dickinson). 11 colonies were randomly selected, and 16S rRNA DNA was PCR amplified using 8F and 1543R universal 16S rRNA primers. PCR products were sequenced (Sanger sequencing) and *Lactobacillus* species were identified using BLAST against the NCBI nonredundant nucleotide and 16S rRNA databases. *Lactobacillus* isolates were stored in MRS media with 20% glycerol at –80°C. For oral gavage, *Lactobacillus* strain Q1-7 was grown in MRS broth and concentrated by centrifugation at 8,000g for 5min. Mice were orally gavaged with $5x10^9$ cfu *Lactobacillus* strain Q1-7 resuspended in 100 μL of saline six days a week.

Fecal microbiota transplantation

Antibiotics (vancomycin hydrocholoride (5 mg/ml), metronidazole (10 mg/ml), ampicillin (10mg/ml), and neomycin trisulfate salt hydrate (10 mg/ml)) were administered to mice in drinking water for 24 hours. Fresh feces were collected from three to four mice in PBS (supplemented with 0.05% cysteine, 1μg/ml vitamin K, 15% glycerol, 5 μg/ml hemin), gently homogenized, pooled, and passed through a 100-μm cell strainer. The suspension was administered by oral gavage six days a week in mice treated with antibiotics.

Statistical analysis

Data were analyzed using Prism (GraphPad) and are presented as mean±SEM. Statistical significance was determined using the unpaired two-tailed Student's *t* test for single variables and two-way ANOVA for two variables. A *p*-value of <0.05 was considered to be statistically significant.

Supplemental Figures

Figure S2.1. Phenotypic and metabolic characterization of $Tsc1^{f/f}$ and $Tsc1^{f/f}CD11c^{Cre}$ mice. Related to Figure 2.1.
(A) qRT-PCR analysis for *Tsc1* and *Tsc2* mRNAs in day 7 bone marrow-derived dendritic cells (n=6 per genotype; analyzed by t-test). (B, C) Assessment of mTORC1 signaling in day 7 $CD11c^{+}$ bone marrow-derived dendritic cells from $Tsc1^{f/f}$ and $Tsc1^{f/f}CD11c^{Cre}$ mice (n=4-7 per genotype; analyzed by t-test). pS6 median fluorescence intensity (MFI) (B) and $pS6^{+}$ cells (C). (D) Body length of $Tsc1^{f/f}$ and $Tsc1^{f/f}CD11c^{Cre}$ mice at 4 and 16 weeks of age. (n=4-5 per genotype; analyzed by t-test). (E) Oxygen consumption per mouse over 24 hours in 8-week-old $Tsc1^{f/f}$ and $Tsc1^{f/f}CD11c^{Cre}$ mice (n=7-9 per genotype; analyzed by t-test). (F) qRT-PCR analysis of thermogenic genes in BAT tissue of 8-week-old $Tsc1^{f/f}$ and $Tsc1^{f/f}CD11c^{Cre}$ mice (n=7 per genotype; analyzed by t-test). (G) Immunoblot for UCP1 protein for mice on HFD housed at 30°C (n=3-4 per genotype). (H) qRT-PCR analysis for *Pomc* and *Agrp* mRNAs in hypothalamus of 8-week-old $Tsc1^{f/f}$ and $Tsc1^{f/f}CD11c^{Cre}$ mice (n=4 per genotype; analyzed by t-test). Data are presented as mean ± SEM.

Figure S2.1. Phenotypic and metabolic characterization of $Tsc1^{f/f}$ and $Tsc1^{f/f}CD11c^{Cre}$ mice. Related to Figure 2.1.

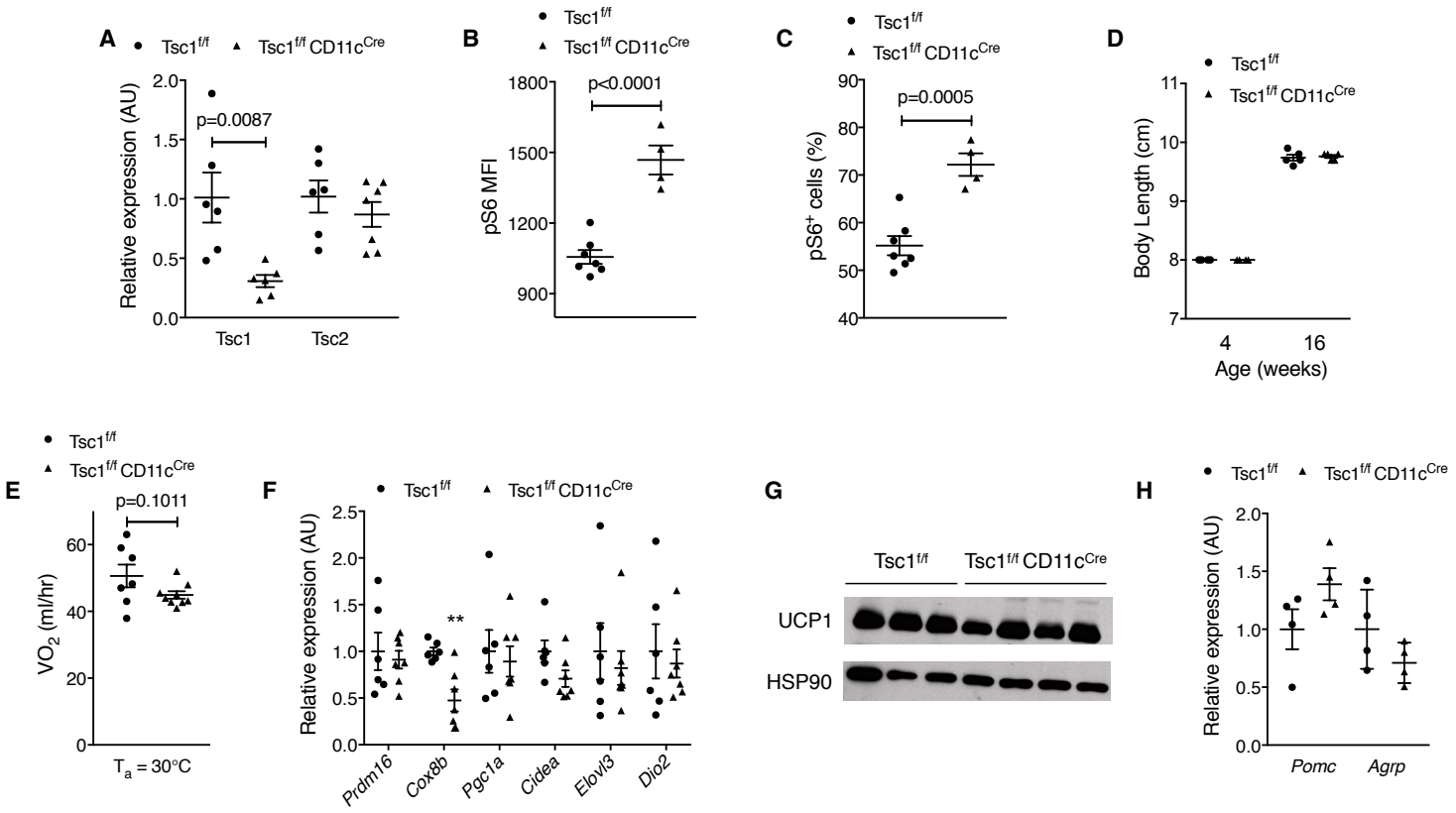

Figure S2.2. Analysis of small intestines and colon of $Tsc1^{f/f}$ and $Tsc1^{f/f}CD11c^{Cre}$ mice. Related to Figure 2.1.

(A) Hematoxylin and eosin staining of representative images of small intestines from $Tsc1^{f/f}$ and $Tsc1^{f/f}CD11c^{Cre}$ mice. (B) Quantification of plasma levels of FITC-Dextran levels 6 hours after oral gavage to $Tsc1^{f/f}$ and $Tsc1^{f/f}CD11c^{Cre}$ mice (n=7-8 per genotype; analyzed by t-test). (C-E) qRT-PCR analysis for tight junction mRNAs in intestines (C), cytokines in mesenteric lymph nodes (mLN) and Peyer's Patches (D), and gut barrier and antimicrobial mRNAs in intestines (E) of 8-week-old $Tsc1^{f/f}$ and $Tsc1^{f/f}CD11c^{Cre}$ mice (n=3-4 per genotype; analyzed by t-test). (F) Spleen mass of 8-week-old $Tsc1^{f/f}$ and $Tsc1^{f/f}CD11c^{Cre}$ mice (n=7 per genotype; analyzed by t-test). Data are presented as mean ± SEM.

Figure S2.2. Analysis of small intestines and colon of Tsc1$^{f/f}$ and Tsc1$^{f/f}$CD11c^{Cre} mice. Related to Figure 2.1.

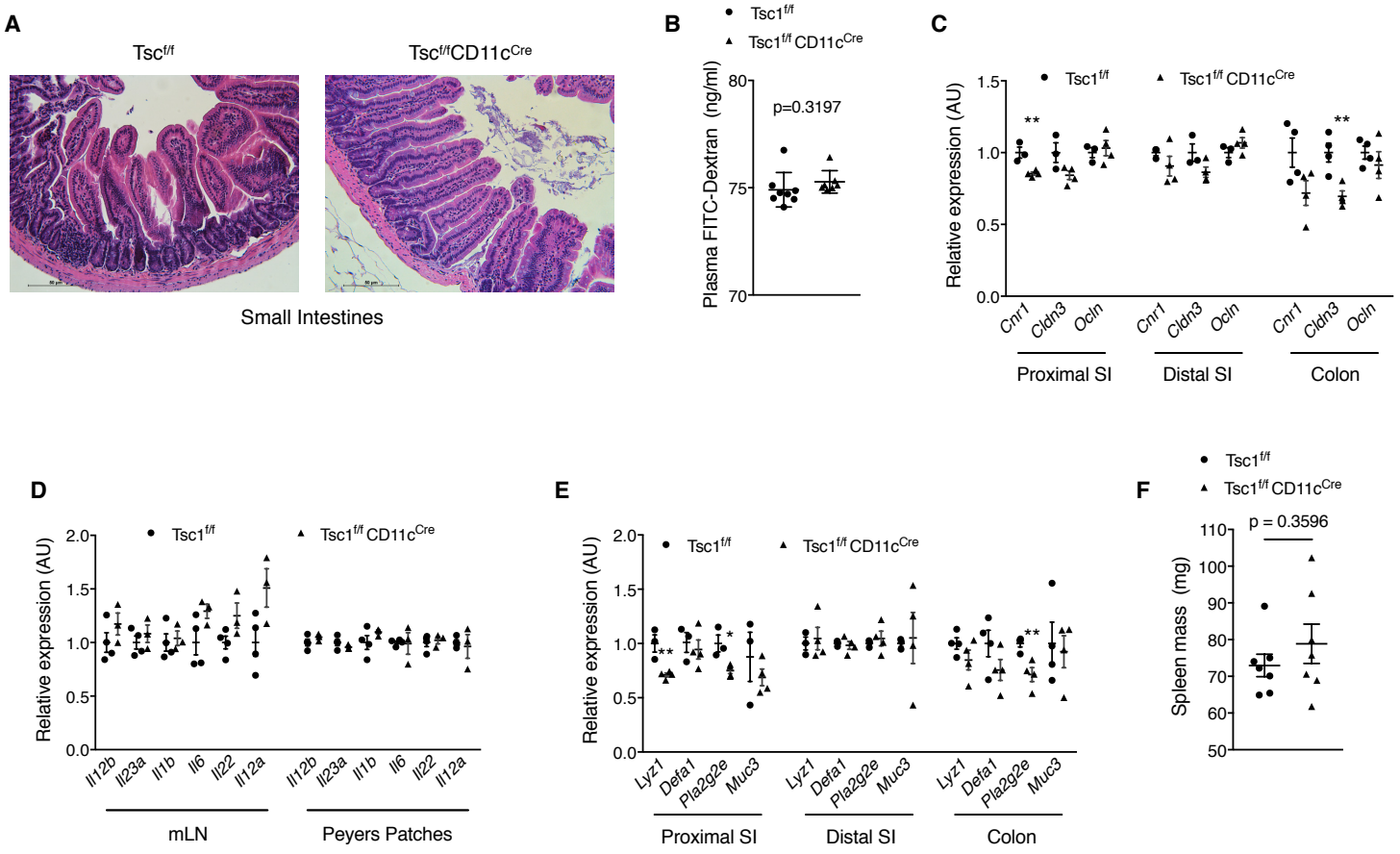

Figure S2.3. Microbiome analysis of $Tsc1^{f/f}$ and $Tsc1^{f/f}CD11c^{Cre}$ mice. Related to Figures 2.2 and 2.3.

(A-C) Plasma levels of leptin (A), and GLP-1 in separately housed (B) and cohoused (C) $Tsc1^{f/f}$ and $Tsc1^{f/f}CD11c^{Cre}$ mice (n=8 per genotype for leptin and n=4-8 per genotype for GLP-1).
(D) Principal Coordinates Analysis (PCoA) of Bray Curtis dissimilarity for ordination of microbial communities of $Tsc1^{f/f}$ and $Tsc1^{f/f}CD11c^{Cre}$ mice cohoused or housed separately after weaning. Each data point represents a single mouse at 8 weeks of age (n=15-19 per genotype; analyzed by ADONIS; p=0.0001, R2=0.255 comparing separately-housed $Tsc1^{f/f}CD11c^{Cre}$ mice to separately-housed $Tsc1^{f/f}$ mice and co-housed mice). (E) Schematic outline for isolation of *Lactobacillus strain Q1-7* from stool of $Tsc1^{f/f}$ mice. (F, G) Changes in abundance of *Rikenellaceae* RC9 group (F) and *Muribaculaceae* group (G) during microbiome chase of $Tsc1^{f/f}CD11c^{Cre}$ mice (n = 2 per chase group; error bars represent range; analyzed by linear mixed effects model FDR<0.1). The dashed lines denote the duration of the microbiome chase. (H) Quantification of cecal, fecal, and plasma metabolites by NMR (n=7 per genotype; analyzed by Mann-Whitney), *p < 0.05.

Figure S2.3. Microbiome analysis of Tsc1$^{f/f}$ and Tsc1$^{f/f}$CD11c^{Cre} mice. Related to Figures 2.2 and 2.3.

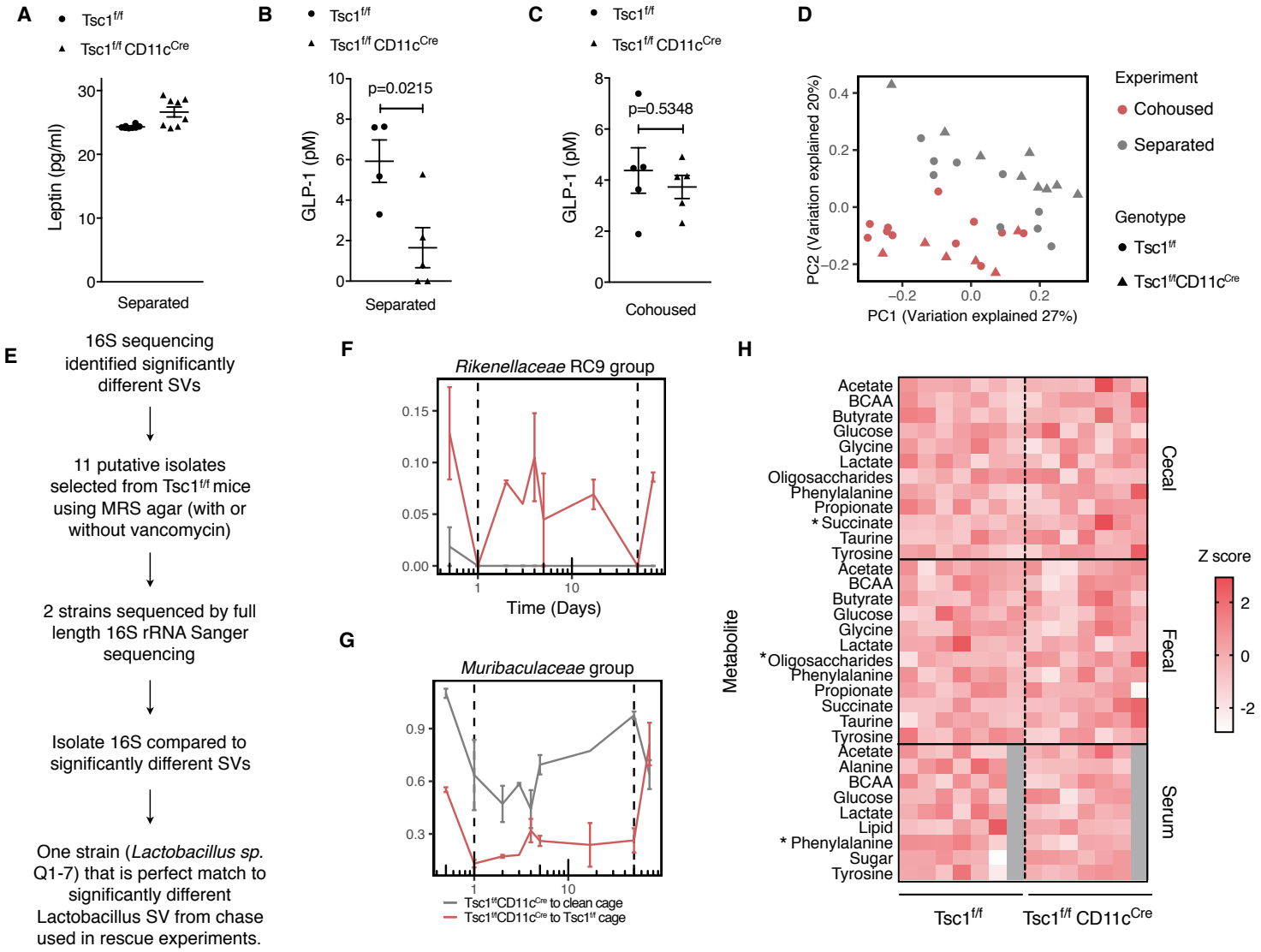

Figure S2.4. Flow cytometric analysis of intestinal immune cells in lamina propria of of $Tsc1^{f/f}$ and $Tsc1^{f/f}CD11c^{Cre}$ mice. Related to Figure 2.4.

(A, B) Quantification by flow cytometry of macrophage and dendritic cell subsets in colon (A) and small intestines (B) of 8-week-old $Tsc1^{f/f}$ and $Tsc1^{f/f}CD11c^{Cre}$ mice (n=3-9 per genotype; analyzed by t-test). (C) Quantification of Peyer's Patches (PPs) and intestinal lymphoid structures (ILS) in distal small intestines of 8-week-old $Tsc1^{f/f}$ and $Tsc1^{f/f}CD11c^{Cre}$ mice (n=9 per genotype; analyzed by t-test). (D) Assessment of mTORC1 signaling by intracellular staining for pS6 in $CD45^{+}CD11c^{+}$ cells isolated from intestinal lamina propria of $Tsc1^{f/f}$ and $Tsc1^{f/f}CD11c^{Cre}$ mice (n=4-6 per genotype; analyzed by t-test). (E) Percent CD4 and CD8 active (CD69+) and proliferated T cells. (n=3 per genotype; analyzed by t-test). Data are presented as mean ± SEM.

Figure S2.4. Flow cytometric analysis of intestinal immune cells in lamina propria of of $Tsc1^{f/f}$ and $Tsc1^{f/f}CD11c^{Cre}$ mice. Related to Figure 2.4.

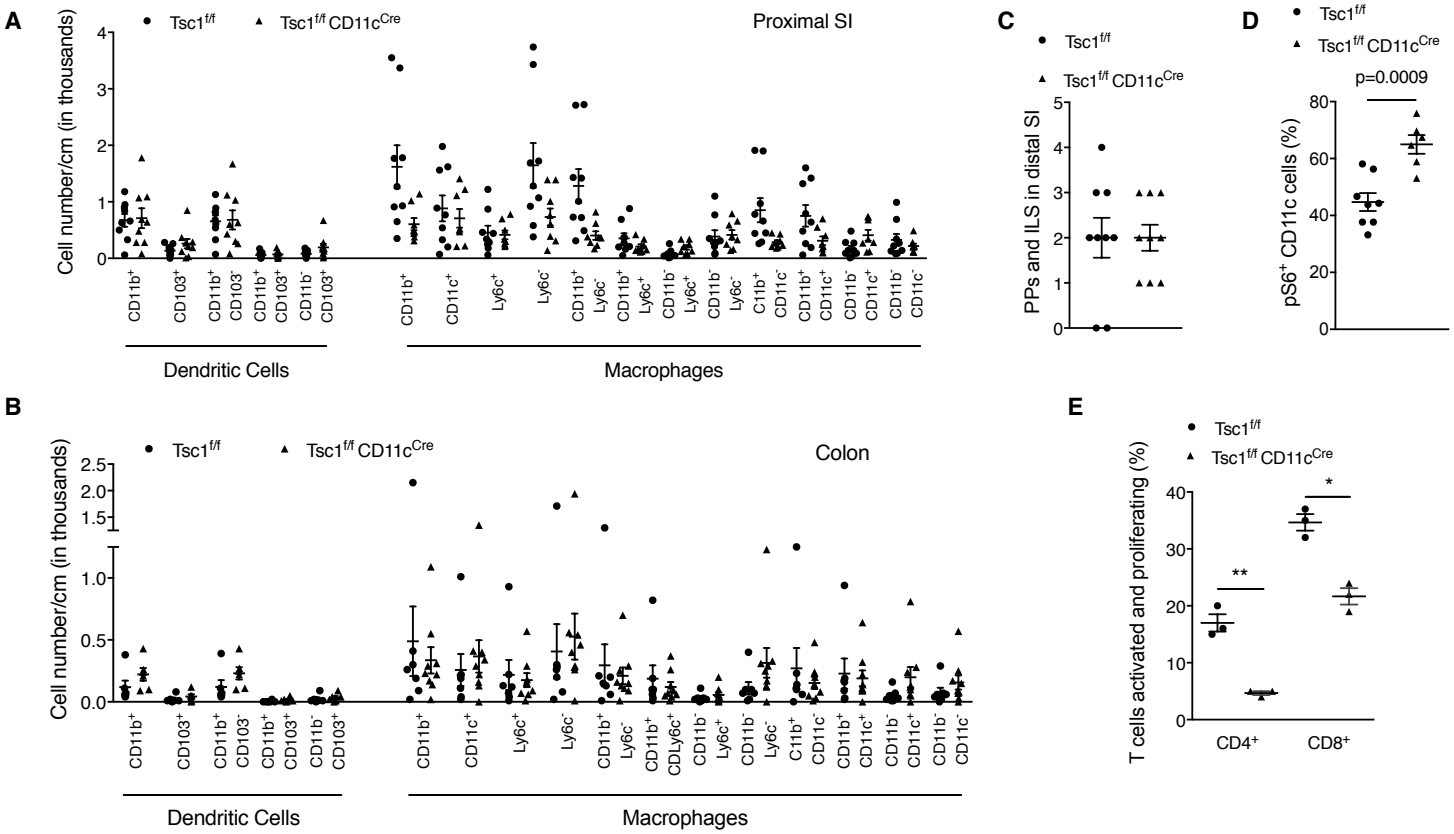

CHAPTER 3.

The role of housing temperature and diet on $Tsc1^{f/f}CD11c^{Cre}$ mice.

ABSTRACT

Thermoneutral housing has been implicated as playing an important role in mouse physiology. However, it is not known what the effect of housing temperature is on insulin sensitivity and weight gain. In addition it is unknown what the effect of housing temperature is on microbial transfer of phenotypes. Here we show that in $Tsc1^{f/f}CD11c^{Cre}$ mice, thermoneutral housing uncouples the reduced weight phenotype from insulin sensitivity when mice are exposed to a high-fat diet. In normal-chow diet mice, room temperature uncouples the reduced weight phenotype from sufficiency of the $Tsc1^{f/f}CD11c^{Cre}$ microbiome to transfer this phenotype. Together our findings reveal that the housing temperature of mice is a crucial factor that determines different aspects of metabolic phenotypes, specially weight gain, insulin sensitivity and microbial transfer of phenotypes.

INTRODUCTION

The effect of housing temperature on metabolic and microbial phenotypes in mice is understudied. The majority of mouse studies are performed at room-temperature (22°C), however mice are significantly cold-stressed at this temperature. Thermoneutrality is defined as the temperature for which an organism expends the least amount of energy for warmth or cooling - this thermoneutral zone is 30°C for mice (Tian et al., 2016). C57BL/6 mice housed at 22°C exhibit a two fold increase in energy expenditure and heart rate in order to stay warm compared to mice housed at thermoneutrality (30°C) (Swoap et al., 2008). With such immense differences in energy expenditure between mice housed at room temperature or thermoneutrality, we asked what the consequence of temperature would be on weight gain, insulin sensitivity and the microbiome.

Mice on a high-fat diet develop insulin insensitivity due to an increase in low-grade, chronic inflammation. In particular, inflammatory macrophages are recruited to adipose tissue and lead to the progression of insulin resistance by increased circulation of pro-inflammatory cytokines such as TNFα, MCP-1 and IL-6 (Odegaard and Chawla, 2013; Osborn and Olefsky, 2012). We therefore hypothesized that housing temperature would have an effect on high-fat diet induced weight gain and insulin sensitivity in $Tsc1^{f/f}$ mice and $Tsc1^{f/f}CD11c^{Cre}$ mice.

Another aspect of our phenotype as described in Chapter 2 is the role of the microbiome in protection from weight gain in $Tsc1^{f/f}CD11c^{Cre}$ mice. Although to the best of our knowledge no direct comparison has been done between the microbiomes of thermoneutral (30°C) and room-temperature (22°C) housed mice, Worthmann et al. compared the microbiomes between (30°C) and (6°C) housed mice. From their work we do know that the gut microbiome is significantly altered at the species level between these two temperatures, with lower richness and

a decreased Shannon index occurring at cold exposure (Worthmann et al., 2017). We therefore hypothesized that the housing temperature of the host has an impact on the microbiome and its sufficiency to transfer a phenotype between mice.

Here we tested the hypothesis that altering the housing temperature of mice was sufficient to affect metabolic and microbiome phenotypes. We found that when mice were on a high-fat diet thermoneutrality was sufficient to uncouple protection from weight gain with protection from insulin insensitivity. In addition, when mice were on a low-fat normal chow diet, room temperature was sufficient to uncouple protection from weight gain from sufficiency of the $Tsc1^{f/f}CD11c^{Cre}$ microbiome to transfer the phenotype to C57BL/6 mice. Our findings suggest that housing temperature of mice has an immense impact on both metabolic and microbiome phenotypes.

RESULTS

Activation of mTORC1 signaling in CD11c cells reduces body mass and food intake in high-fat diet fed mice at thermoneutrality.

We first asked if placing $Tsc1^{f/f}CD11c^{Cre}$ mice on a high-fat diet (protein 20%, fat 60%, carbohydrates 20%) while housed at thermoneutrality would recapitulate the phenotype we observed on a low-fat normal chow diet (protein 24.517%, fat 13.134%, carbohydrates 62.349%). We found that even when placed on a high-fat diet, $Tsc1^{f/f}CD11c^{Cre}$ mice still weighed less than $Tsc1^{f/f}$ mice (Figure 3.1A). From Dual-Energy X-ray Absorptiometry (DEXA) we found that these differences were due to decreased fat mass in $Tsc1^{f/f}CD11c^{Cre}$ mice (Figure 3.1B). We next asked if these $Tsc1^{f/f}CD11c^{Cre}$ mice weighed less due to a reduction in food consumption. To do this we measured metabolic parameters for 48 hours in a Comprehensive Lab Animal Monitoring System (CLAMS) chamber. We found that $Tsc1^{f/f}CD11c^{Cre}$ mice consumed less food than $Tsc1^{f/f}$ mice (Figure 3.1C), whereas the other metabolic parameters of oxygen consumption, RER and physical activity (Figure 3.1D-F) were not significantly different.

Thermoneutrality uncouples reduced weight gain from insulin intolerance $Tsc1^{f/f}CD11c^{Cre}$ mice on a high-fat diet.

Housing temperature has been shown to have a large effect on numerous metabolic parameters in mice . We next wanted to ask if and how temperature would affect the metabolic phenotypes of $Tsc1^{f/f}CD11c^{Cre}$ mice on a high-fat diet. We first established that $Tsc1^{f/f}CD11c^{Cre}$ mice still weighed less compared to $Tsc1^{f/f}$ mice when housed at 22°C and on a high-fat diet (Figure 3.2A). One characteristic of mice on a high-fat diet is diet induced insulin insensitivity. We therefore asked what the effect of temperature on insulin insensitivity was in $Tsc1^{f/f}CD11c^{Cre}$

mice. Glucose and insulin tolerance tests revealed that $Tsc1^{f/f}CD11c^{Cre}$ mice were protected from high-fat diet induced insulin insensitivity at 30°C (Figure 3.2C and E) but not at 22°C (Figure 3.2C and E). As fasting time and glucose dosage can affect glucose-tolerance test outcomes, we asked if altering either of these would result in insulin sensitivity differences at 30°C . Even a shorter fasting time (6 hours versus overnight) and a higher dosage of glucose (1g/kg versus 1.5g/kg) did not result in insulin sensitivity differences between $Tsc1^{f/f}CD11c^{Cre}$ and $Tsc1^{f/f}$ mice housed at 30°C (Figure S3.1A-B).

The $Tsc1^{f/f}CD11c^{Cre}$ microbiome is sufficient to confer a reduced weight gain phenotype to C57BL/6 mice only at thermoneutrality, not at room temperature.

We next examined the effect of temperature on the microbiome of $Tsc1^{f/f}CD11c^{Cre}$ mice. The reduced weight phenotype in $Tsc1^{f/f}CD11c^{Cre}$ mice relative to $Tsc1^{f/f}$ mice holds independent of housing temperature (Figure 3.2F). We then asked if housing temperature affected the sufficiency of the $Tsc1^{f/f}CD11c^{Cre}$ microbiome to transfer the reduced weight phenotype to C57BL/6 mice . We tested this by gavaging antibiotic treated C57BL/6 mice with stool from $Tsc1^{f/f}CD11c^{Cre}$ mice or $Tsc1^{f/f}$ mice. We found that the microbiome in stool from $Tsc1^{f/f}CD11c^{Cre}$ mice was sufficient to cause a reduced weight phenotype only in C57BL/6 mice housed at 30°C (Figure 3.2G) but not in C57BL/6 mice housed at 22°C (Figure 3.2H).

In summary this chapter elucidates how temperature and diet affect metabolic and microbial phenotypes of $Tsc1^{f/f}CD11c^{Cre}$ mice. When mice are on a high-fat diet, thermoneutrality uncouples insulin sensitivity from the reduced weight gain phenotype. When mice are on a low-fat diet, room temperature uncouples the microbiome sufficiency from weight phenotype (Figure 3.3).

DISCUSSION

This chapter has established the role of housing temperature on metabolic and microbiome phenotypes. Thermoneutrality uncouples reduced weight gain from insulin sensitivity in mice on a high-fat diet. Immune cell infiltrates in epididymal fat causes insulin resistance in high-fat diet fed mice (Shoelson et al., 2006). Future work will therefore examine differences in epididymal fat pad immune cell populations. This will be done by flow cytometric analysis of $CD11c^{+}$ cell, T and B-cell subsets.

Room temperature uncouples protection from weight gain with microbiome sufficiency to transfer a phenotype. This suggests that the microbiomes of mice housed at 30°C and 22°C are different and that different mechanisms are resulting in the same phenotype depending on housing temperature. $Tsc1^{f/f}CD11c^{Cre}$ mice are protected from weight gain at both 30°C and 22°C but the underlying microbiome changes that result in this could be different. 16S sequencing of stool from both $Tsc1^{f/f}$ mice and $Tsc1^{f/f}CD11c^{Cre}$ mice will be performed. To further examine the effect of temperature on transfer of phenotype through the microbiome future work will treat C57BL/6 mice housed at 30°C and 22°C with stool from $Tsc1^{f/f}CD11c^{Cre}$ mice housed at 30°C and 22°C (Figure 3.4). If C57BL/6 mice housed at 30°C weigh less when given stool from 22°C housed $Tsc1^{f/f}CD11c^{Cre}$ mice then this indicates that thermoneutrality housed C57BL/6 mice are "universal acceptors" regardless of donor temperature. If however the weight phenotype does not transfer then this indicates that a match between donor and recipient housing temperature is needed. If C57BL/6 mice housed at 22°C weigh less when given stool from 22°C housed $Tsc1^{f/f}CD11c^{Cre}$ mice this this indicates that a match between donor and recipient housing temperature is needed. If however there is no weight difference then this indicates that the mechanism of the microbiome in this phenotype is temperature specific. That

is, the microbiome is sufficient to cause weight changes between $Tsc1^{f/f}$ and $Tsc1^{f/f}CD11c^{Cre}$ mice only at thermoneutrality. If this were the case then this underscores the importance of understanding the fundamental differences between the microbiomes of mice housed at room temperature and thermoneutrality, an area that has not yet been explored.

The microbiome of mice on a high-fat diet is drastically different from that of mice on a low-fat normal diet (Ley et al., 2005) . Therefore, another further aspect yet to be explored is the role of the microbiome in high-fat diet fed mice. All studies listed above will therefore be performed on mice fed a high-fat diet. Is the reduced weight in $Tsc1^{f/f}CD11c^{Cre}$ mice also dependent on the microbiome when mice are on a high-fat diet? And is this microbiome sufficient to transfer the phenotype of these mice housed at either thermoneutrality or room-temperature? In conclusion, this chapter highlights the important role diet and housing temperature play on metabolic and microbial phenotypes and mechanisms.

REFERENCES

Ley, Ruth E., et al. "Obesity alters gut microbial ecology." Proceedings of the National Academy of Sciences 102.31 (2005): 11070-11075.

Odegaard, Justin I., and Ajay Chawla. "The immune system as a sensor of the metabolic state." Immunity 38.4 (2013): 644-654.

Osborn, Olivia, and Jerrold M. Olefsky. "The cellular and signaling networks linking the immune system and metabolism in disease." Nature medicine 18.3 (2012): 363.

Shoelson, S.E., Lee, J., and Goldfine, A.B. (2006). Inflammation and insulin resistance. The Journal of Clinical Investigation *116*.

Swoap, Steven John, et al. "Vagal tone dominates autonomic control of mouse heart rate at thermoneutrality." American Journal of Physiology-Heart and Circulatory Physiology (2008).

Tian, Xiao Yu, et al. "Thermoneutral housing accelerates metabolic inflammation to potentiate atherosclerosis but not insulin resistance." Cell metabolism 23.1 (2016): 165-178.

Worthmann, Anna, et al. "Cold-induced conversion of cholesterol to bile acids in mice shapes the gut microbiome and promotes adaptive thermogenesis." Nature medicine 23.7 (2017): 839.

FIGURE LEGENDS

Figure 3.1. $Tsc1^{f/f}CD11c^{Cre}$ mice on a high-fat diet and housed at thermoneutrality weigh less and consume less food than $Tsc1^{f/f}$ mice.
(A) Change in body mass over time of mice placed on a high-fat diet at 6 weeks of age while housed at thermoneutrality (n=6-8 per genotype; analyzed by two-way ANOVA) (B) Dual-energy X-ray absorptiometry of mice from (A) after 12 weeks of HFD (n=3-5 per genotype; analyzed by t-test). (C-F) Metabolic analysis of food intake (C), oxygen consumption (D), RER (E) and total activity (F) of thermoneutrally housed mice after 12 weeks on a HFD (n=3 per genotype; analyzed by t-test or by two-way ANOVA).

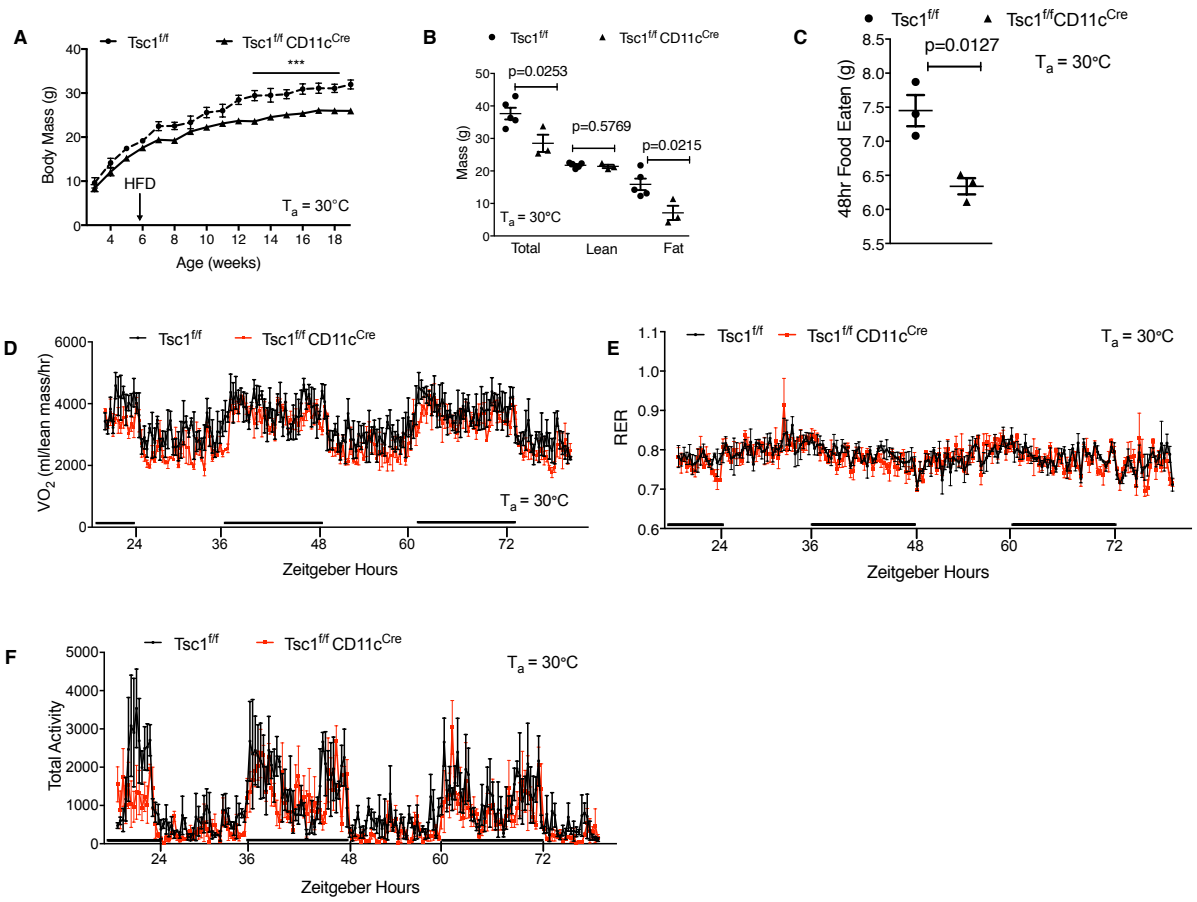

Figure 3.1. Tsc1$^{f/f}$CD11c^{Cre} mice on a high-fat diet and housed at thermoneutrality weigh less and consume less food than Tsc1$^{f/f}$ mice.

Figure 3.2. Thermoneutrality uncouples reduced weight gain from insulin intolerance and microbiome sufficiency in $Tsc1^{f/f}CD11c^{Cre}$ mice.
(A) Change in body mass over time of mice placed on a high-fat diet while housed at 22°C (n=5 per genotype; analyzed by two-way ANOVA). (B-C) Glucose-tolerance tests for mice on a high-fat diet housed at room temperature (B) and thermoneutrality (C). Mice were fasted overnight and administered 1.5g/kg glucose. (n=4-5 per genotype; analyzed by two-way ANOVA). (D-E) Insulin-tolerance tests of mice on a high-fat diet housed at room temperature (D) and thermoneutrality (E) (n=4-5 per genotype; analyzed by two-way ANOVA). (F) 13-week old body weight of $Tsc1^{f/f}$ or $Tsc1^{f/f}CD11c^{Cre}$ mice on a low-fat normal chow diet housed at either 30°C or 22°C (n = 4-5 per genotype; analyzed by t-test). (G-H) % weight gain in C57BL/6J mice given stool from either $Tsc1^{f/f}$ or $Tsc1^{f/f}CD11c^{Cre}$ mice housed at 30°C (G) or 22°C (H) (n=7-8 per genotype; analyzed by t-test).

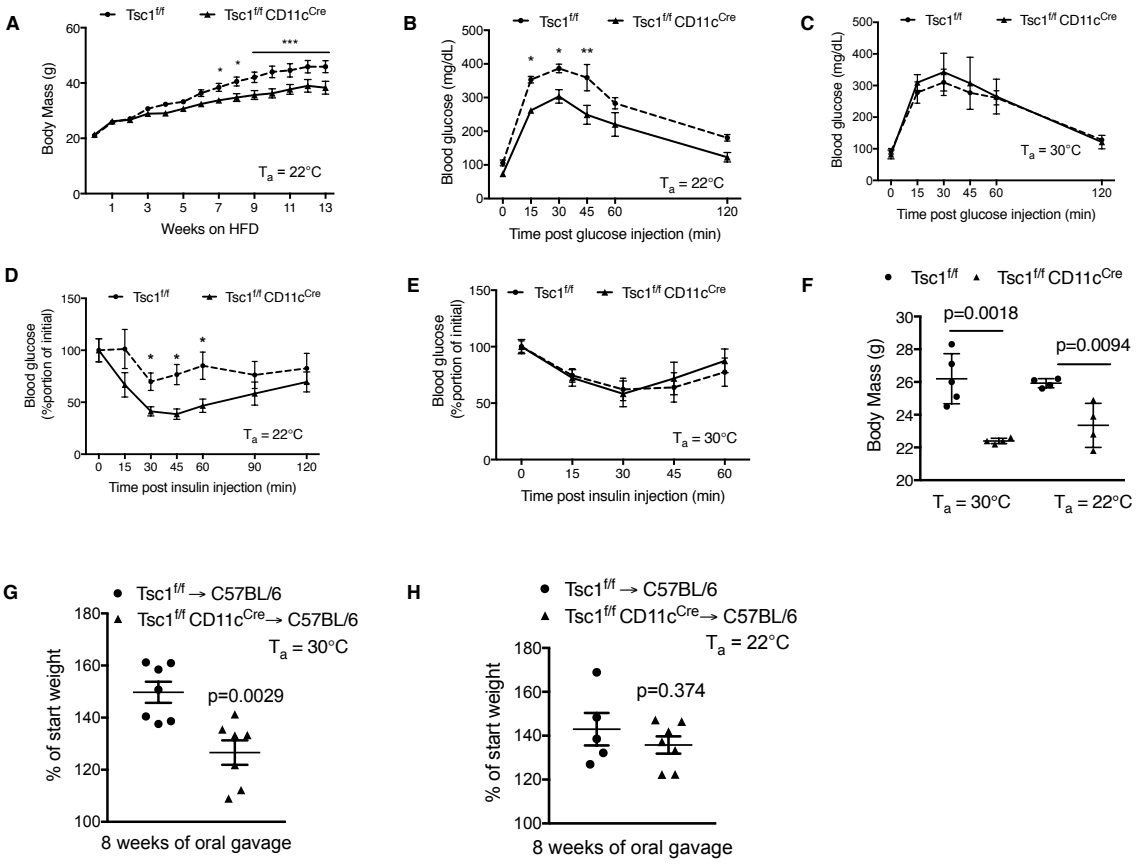

Figure 3.2. Thermoneutrality uncouples reduced weight gain from insulin intolerance and microbiome sufficiency in $Tsc1^{f/f}CD11c^{Cre}$ mice.

Figure 3.3. Summary of the effects of housing temperature and diet on weight gain, insulin sensitivity and microbiome sufficiency phenotypes in $Tsc1^{f/f}CD11c^{Cre}$ mice relative to $Tsc1^{f/f}$mice .

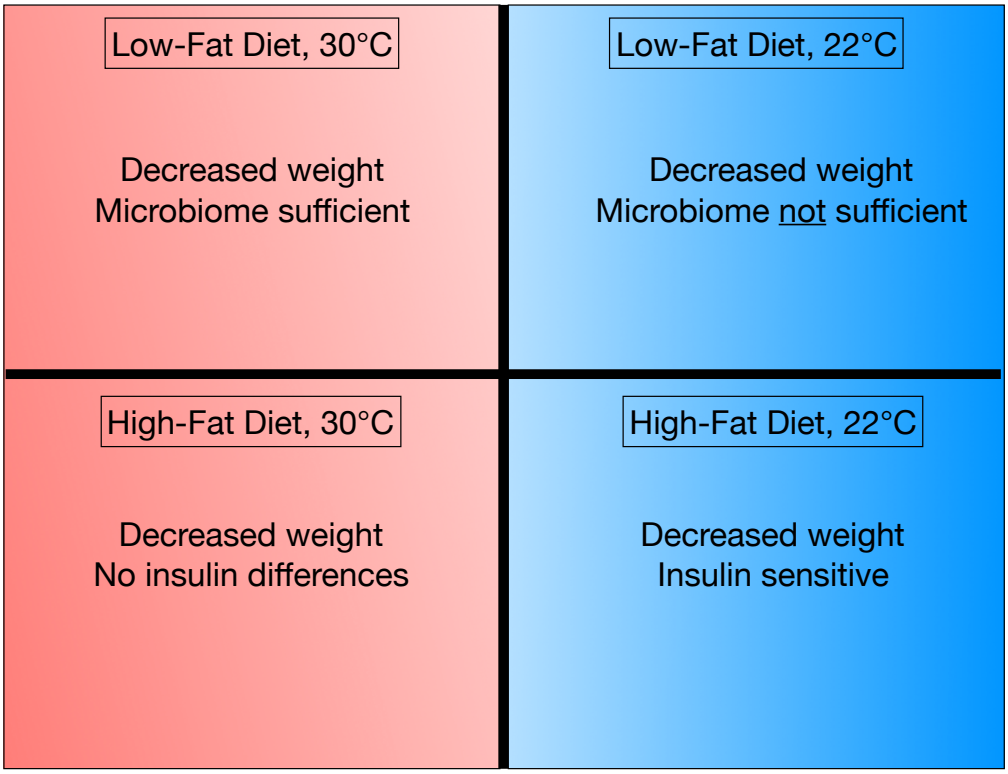

Figure 3.3. Summary of the effects of housing temperature and diet on weight gain, insulin sensitivity and microbiome sufficiency phenotypes in $Tsc1^{f/f}CD11c^{Cre}$ mice relative to $Tsc1^{f/f}$mice .

Figure S3.1. Fasting times and glucose dosage do not restore glucose tolerance differences in $Tsc1^{f/f}CD11c^{Cre}$ mice.
(A-B) Glucose-tolerance tests of mice on a high-fat diet housed at thermoneutrality. (A) Mice were fasted for 6 hours and administered 1.5g/kg glucose. (B) Mice were fasted for 6 hours and administered 1g/kg glucose (n=4-5 per genotype; analyzed by two-way ANOVA).

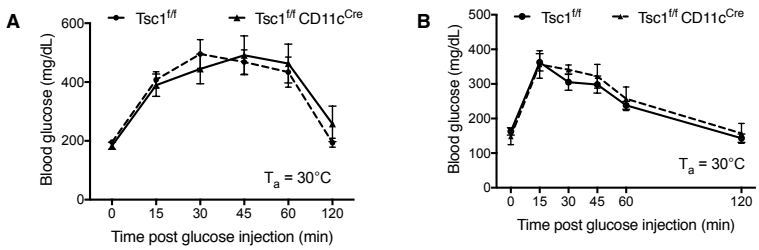

Figure S3.1. Fasting times and glucose dosage do not restore glucose tolerance differences in $Tsc1^{f/f}CD11c^{Cre}$ mice.

Figure 3.4. Summary of known and potential housing temperature effects on the $Tsc1^{f/f}CD11c^{Cre}$ microbiome sufficiency to transfer reduced weight phenotype to C57BL/6J mice.

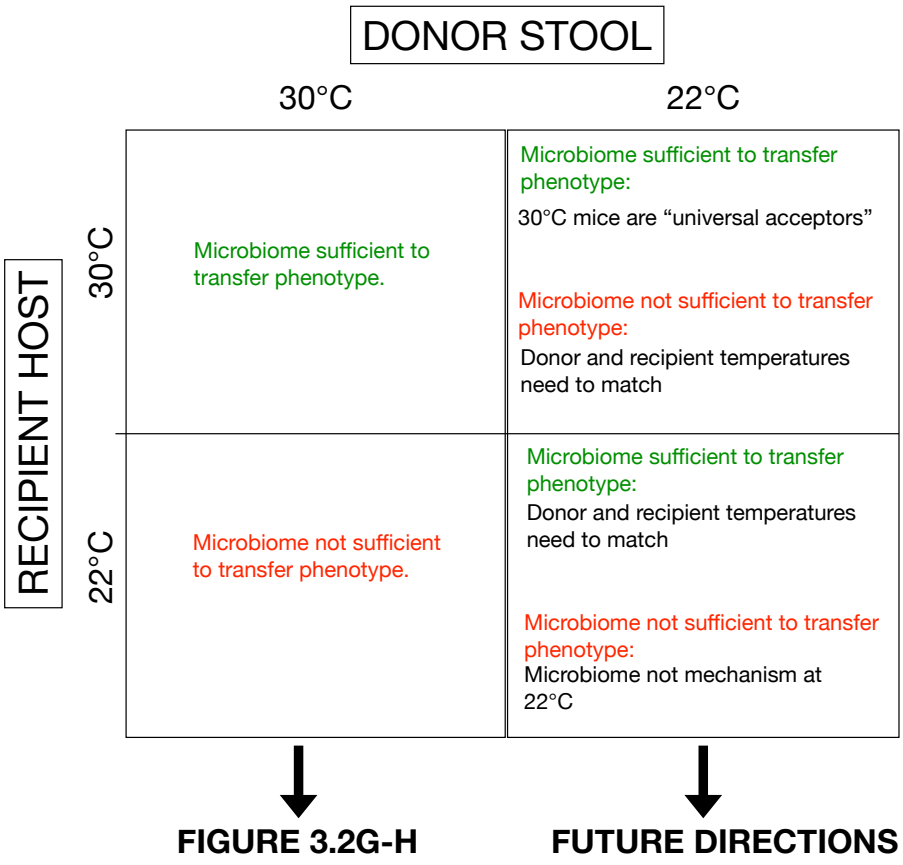

MATERIALS AND METHODS

Animal studies

Mice were maintained in the University of California San Francisco specific pathogen–free animal facility in accordance with the guidelines established by the Institutional Animal Care and Use Committee and Laboratory Animal Resource Center. Mice were housed either at 30°C after weaning or kept at 22°C in Darwin or Power Scientific environmental chambers under a 12-hr light:dark cycle. $Tsc1^{f/f}$ and $CD11c^{Cre}$ mice were purchased from Jackson Laboratories, backcrossed onto C57BL/6J background (*Nnt* null) for 10 generations, and used to generate $Tsc1^{f/f}$ $CD11c^{Cre}$ mice. Mice were fed normal chow diet (5053, Pico labs) or high fat diet (D12492i, Research Diets)

Energy expenditure and body composition analysis

Body composition (fat and lean mass) analysis were performed on anesthetized mice using Dual-energy X-ray absorptiometry (DEXA). For measurement of energy expenditure, food intake, and locomotor activity, mice were placed in CLAMS (Columbus Instruments) cages that housed an environmental chamber set at 30°C. After acclimatization for one day, data on oxygen consumption, locomotor activity, and food intake was collected every 22 minutes.

Glucose and insulin tolerance tests

For glucose and insulin tolerance tests, mice were intraperitoneally injected with glucose (1 or 1.5g/kg of body weight) after 6h or 14h fast or insulin (1U/kg of body weight) after 6h or overnight fast, and blood glucose was measured at regular intervals using tail blood.

Fecal microbiota transplantation and Germ-free colonization

Antibiotics (vancomycin hydrocholoride (5mg/ml), metronidazole (10mg/ml), ampicillin (10mg/ml), and neomycin trisulfate salt hydrate (10 mg/ml)) were administered to mice in drinking

water for 24 hours. Fresh feces were collected from three to four mice in 0.1mg/ μL PBS (supplemented with 0.05% cysteine, 1μg/ml vitamin K, 15% glycerol, 5 μg/ml hemin), gently homogenized, pooled, and passed through a 100-μm cell strainer. The suspension was administered by oral gavage six days a week in mice treated with antibiotics.

Statistical analysis

Data were analyzed using Prism (GraphPad) and are presented as mean±SEM. Statistical significance was determined using the unpaired two-tailed Student's *t* test for single variables and two-way ANOVA followed by Bonferroni post-tests for two variables. A *p*-value of <0.05 was considered to be statistically significant.

CHAPTER 4.

CONCLUDING REMARKS AND FUTURE DIRECTIONS

Overall this body of work shows that nutrient sensing in immune cells regulates systemic metabolism through the microbiome and that this interaction is influenced by housing temperature and diet.

This body of work raises some interesting questions. From Chapter 2, one is left wondering what are the mechanisms by which *Lactobacillus johnsonii Q1-7* controls food intake and weight gain. To address this we will first need to understand if *Lactobacillus johnsonii Q1-7* uniquely rescues $Tsc1^{f/f}CD11c^{Cre}$ mice. This can be done by gavaging different members of the Lactobacillus genus and classifying them into groups that are either able to rescue or to not rescue the phenotype. One can then perform comparative genomic analysis on species in either group to understand what is unique and therefore have a better understanding of the properties of Lactobacillus responsible for rescuing the weight and food consumption differences in $Tsc1^{f/f}CD11c^{Cre}$ mice. In conjunction one can perform metabolomics on the serum of $Tsc1^{f/f}CD11c^{Cre}$ mice before and after rescue by *Lactobacillus johnsonii Q1-7* to understand what metabolites may be changing pre and post rescue and if any of those are directly made by *Lactobacillus* based on the genome analysis. The second major question is exactly how $CD11c^{+}$ cells are influencing IgA binding to *Lactobacillus johnsonii Q1-7.* In order to assess this the $Tsc1^{f/f}CD11c^{Cre}$ and $Tsc1^{f/f}$ mice would have to re-derived under germ-free conditions and mono-colonized with *Lactobacillus johnsonii Q1-7*. IgA binding can then be analyzed under these conditions more specifically.

From Chapter 3 one major question is how the microbiome changes under different housing conditions – our work suggests that the $Tsc1^{f/f}CD11c^{Cre}$ mice microbiome changes with housing temperature but this needs to be analyzed. To assess this, littermate controls from

$Tsc1^{f/f}CD11c^{Cre}$ and $Tsc1^{f/f}$ mice would be bred at room-temperature and then one cohort moved to thermoneutrality and 16S sequencing performed on stool weekly to assess how the microbiome changes with housing temperature over time. In addition the other major question that this work raises is how the rescue of this phenotype performs under high-fat diet conditions – what is different or similar between different dietary conditions?

Publishing Agreement

It is the policy of the University to encourage the distribution of all theses, dissertations, and manuscripts. Copies of all UCSF theses, dissertations, and manuscripts will be routed to the library via the Graduate Division. The library will make all theses, dissertations, and manuscripts accessible to the public and will preserve these to the best of their abilities, in perpetuity.

Please sign the following statement:

I hereby grant permission to the Graduate Division of the University of California, San Francisco to release copies of my thesis, dissertation, or manuscript to the Campus Library to provide access and preservation, in whole or in part, in perpetuity.

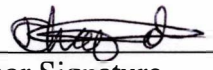

Author Signature

12/10/18

Date